Estimation of Satellite Rainfall Error Variance Using Readily Available Geophysical Features

Abebe S. Gebregiorgis and Faisal Hossain

Abstract—**The present study addresses the estimation of error variance (mean square error, MSE) of three satellite rainfall products: i) Tropical Rainfall Measuring Mission (TRMM) Multi-satellite Precipitation Analysis (TMPA) product of 3B42RT; ii) Climate Prediction Center (CPC) Morph (CMORPH); and iii) Precipitation Estimation from Remotely Sensed Information using Artificial Neural Networks-Cloud Classification System (PERSIANN-CCS). Nonlinear regression model is used to fit the response variable (satellite rainfall error variance) with explanatory variable (satellite rainfall rate) by grouping them as function of three key geophysical features: topography, climate, and season. The results of the study suggest that the error variance of a rainfall product is strongly correlated with rainfall rate and can be expressed as a power-law function. The geophysical feature based error classification analysis helps in achieving superior accuracy for prognostic error variance quantification in the absence of ground truth data. The multiple correlation coefficients between the estimated and observed error variance over an independent validation region (Upper Mississippi River basin) and time period (2007–2010) are found to be 0.75, 0.86, and 0.87 for 3B42RT, CMORPH, and PERSIANN-CCS products, respectively. In another validation region (Arkansas-Red River basin), the correlation coefficients are 0.59, 0.89, and 0.92 for the same products, respectively. Results of the assessment of error variance models reveal that the type of error component present in a satellite rainfall product directly impacts the accuracy of estimated error variance. The model estimates the error variance more accurately when the precipitation error components are mostly hit bias or false precipitation, while for a product with extensive missed precipitation, the accuracy of estimated error variance is significantly compromised. The study clearly demonstrates the feasibility of quantifying the error variance of satellite rainfall products in a spatially and temporally varying manner using readily available geophysical features and rainfall rate. The study is a path finder to a globally applicable and operationally feasible methodology for error variance estimation at high spatial and temporal scales for advancing satellite rainfall applications in ungauged basins.**

Index Terms—**Climate, error variance, geophysical features, rainfall rate, regression model, satellite rainfall, season, topography.**

I. Introduction

SATELLITE precipitation estimation has made considerable progress over the last few decades in terms of accuracy, resolution, and global coverage (hereafter the word "precipitation" will be used interchangeably with "rainfall"). It has developed from the archaic Global Precipitation Climatology Project (GPCP) [1]–[4] to the present variety of higher resolution rainfall products such as the TRMM Multi-satellite Precipitation Analysis (TMPA) [5]; CMORPH [6], [7]; PERSIANN-CCS [8]; PERSIANN [9]; Rain Estimation Using Forward-Adjusted Advection of Microwave Estimates (REFAME) [10]; and Global Satellite Mapping of Precipitation (GSMaP) [11].

The resolution of satellite rainfall data has also improved from one degree spatial and monthly time scale available in the 1990s to the 0.25° and 3 hourly or higher spatial and temporal scales, respectively which is available today. Through this evolution, satellite rainfall data has made a significant contribution to understanding of the dynamics of earth's climatic and hydrologic system. Global rainfall data is nowadays routinely produced using a range of variety of satellite retrieval algorithms and techniques [5]–[8], [10], [11] and available for the users and scientific communities. Despite the weakness it may have, satellite rainfall has become indispensible for hydrologic simulation and climate prediction especially where there is no ground observation data.

Uncertainty in satellite rainfall products however remains inherent because of the fundamental constraint posed by the indirect approach of remote sensing. To tackle this inherent shortcoming, numerous approaches have been developed to reduce uncertainty of satellite rainfall estimation. Among the many, some common approaches are: combining multisensors infrared (IR) and microwave (MW) data [5], [12]; merging multi-satellite products with gauge observation [4], [13]; implementing different rainfall screening and retrieval techniques [14], [6], [8]; blending (or merging) different satellite rainfall products based on *a priori* (diagnostic) hydrologic predictability [15]; fusion of multiscale multisensor precipitation using Gaussian-scale mixtures in the wavelet domain [16]. Regardless of such efforts, non-negligible errors associated with the satellite rainfall products still remains a challenge. There always seems to be room to improve the quality of satellite rainfall data sets [9], [17], [18].

One approach, to aid the application of satellite rainfall data for hydrologic predictions, is to understand the characteristics of errors and their outcomes in hydrologic modeling under various possible scenarios [19]–[21]. As the usefulness of these rainfall data sets relies on users' knowledge of uncertainty about the product, operational quantification of satellite rainfall uncertainty is a pressing need among data producers and users [22]. The issue of quantitative analysis of uncertainty can easily be addressed in a location where quality-controlled ground observation data is adequately available. However, most parts

Manuscript received August 9, 2013; revised November 30, 2013; accepted January 1, 2013. This work was supported by the NASA Earth and Space Fellowship awarded to the first author and the NASA New Investigator Award (NNXAR32G) awarded to the second author.

The authors are with the Tennessee Technological University, Cookeville, TN 38505 USA (e-mail: abesine2002@gmail.com; fhossain@tntech.edu).

Color versions of one or more of the figures in this paper are available online at http://ieeexplore.ieee.org.

Digital Object Identifier 10.1109/TGRS.2013.2238636

of the globe are sparse regions that are not well-covered by gauges or ground radars and others cannot be observed by ground networks (e.g., large water bodies, mountainous and remote desert areas). Therefore, the question is *how one can estimate the uncertainty of a satellite rainfall product at any location and time in the absence of ground validation data*?

In the past few years, several studies have been reported on satellite rainfall uncertainty [19], [20], [22]–[37]. The main foci of these studies were on investigation of error characteristics, quantification of errors, and propagation and impacts of uncertainty on hydrologic model simulations. Huffman [22] was perhaps the first in formulating a functional relationship for RMS random error using the average rainfall rate and probability distribution parameters associated with the precipitation estimates. The RMS random error investigated in the study was a combination of both sampling and algorithmic error, and it was directly proportional to the rainfall rate as shown in

$$\sigma = \frac{\overline{r}}{N_1}\left(\frac{H-p}{p}\right)^{0.5} \tag{1}$$

where $\overline{r}$ is the space–time average of precipitation over set of E, H is a function of the shape of probability distribution of precipitation (approximately 1.5 for most of global), p is the frequency of nonzero precipitation in set E, and N_1 is the number of independent samples in E. The estimated RMS was found to be reasonably comparable to the observed RMS error [38]. The study considered 2.5° spatial and monthly temporal scales to compute the RMS error [22].

Steiner [34] developed a framework to express the sampling error variance of radar rainfall estimate as function of rainfall rate R, domain size A, time T, and sampling interval Δt per

$$\sigma = f\left(\frac{1}{R}, \frac{1}{A}, \frac{\Delta t}{T}\right). \tag{2}$$

According to this study, the random error due to sampling was assumed directly proportional to sampling time interval and inversely to size of space and time domain and rainfall rate. In the case of Huffman [22], the direct proportional relation between the total random error (which was a combination of both sampling and measurement-algorithmic errors) and rainfall rate was dominated by the existence of measurement-algorithmic error. This suggested that measurement-algorithmic error was the major component of the total uncertainty and it was directly proportional to the rainfall rate. In the current era of significantly improved temporal sampling by the constellation of passive microwave (PMW) sensors, it is fair to claim that sampling error is now a relatively negligible source of uncertainty at the daily or higher timescales.

To explore the algorithmic uncertainty in detail, Tian and Peters-Lidard [19] developed a global map of satellite rainfall uncertainty (which reflected both systematic and random errors) by computing ensemble mean of six different satellite rainfall products. The standard deviation was computed from the mean (i.e., anomalies) as a measurement of uncertainty. The finding revealed that the uncertainty over the ocean was relatively smaller, as expected, when compared over land. Besides, large amount of uncertainty was observed over high latitude during the cold season. It is clear from past studies that the knowledge of uncertainly inherent in satellite rainfall estimates is important for data users and producers. For instance, Huffman [22] indicated that spatially and temporally varying uncertainty is more important than single data set-averaged estimate. The former helps data producers to evaluate the performance of their algorithms and make the necessary adjustment as a function of location, storm systems and seasons. It also assists data users to assess models' simulation outputs and make more reliable prediction.

However, the nature and magnitude of rainfall errors associated with different satellite rainfall products are not thoroughly investigated and fully addressed to broaden their application at relevant spatial and temporal scales. Unless ground truth data is available, there is no way for the users to know error information associated with 3B42RT, CMORPH, or PERSIANN-CCS products at different part of the globe. Without the fundamental knowledge and guideline on selection of publicly available satellite rainfall products, users rightfully can ask "*which product should one use for a specific hydrological investigation at a particular location? Is there a mechanism for users to know the uncertainty of these products without having access to ground truth data at a specific location*?" This study seeks an answer to the latter question with a view to further promote satellite rainfall products for hydrological application. The study aims at quantifying the error variance of three satellite rainfall products using regression models classified according to easily available geophysical features of the basin and satellite rainfall estimates. Previous studies on estimation of error variance have not leveraged the role played by readily available geophysical features and hence, this study represents a new contribution to the body of knowledge.

The finding of the current study (estimation of spatially and temporally varying error variance using regression model) is also expected to contribute to the merging of various satellite products to a unified state in ungauged basins. Gebregiorgis and Hossain [15], [39] earlier proposed a merging scheme for different satellite rainfall products based on individual performance. The developed merging scheme used error variance of hydrologic predictability to generate weight factors of individual products in the merging process. The finding suggested that leveraging runoff error variance yielded a more accurate merged product [15]. In a follow-up paper, Gebregiorgis and Hossain [39] reported that the use of both spatial and temporal varying error signatures of hydrologic predictability was more useful in merging products for better hydrologic prediction. Therefore, any space–time estimation of error variance over ungauged regions will be valuable in the merging of rainfall products.

In another work, Gebregiorgis and Hossain [27] showed that investigating rainfall uncertainty based on topography, climate regions and seasons is a systematic approach to understanding the nature and magnitude of errors in satellite rainfall products. Topography has a major effect on climate and formation of precipitation. For instance, mountains can affect climate by changing the patterns of temperature, precipitation, and wind circulation. Based on these fundamental drivers, Gebregiorgis

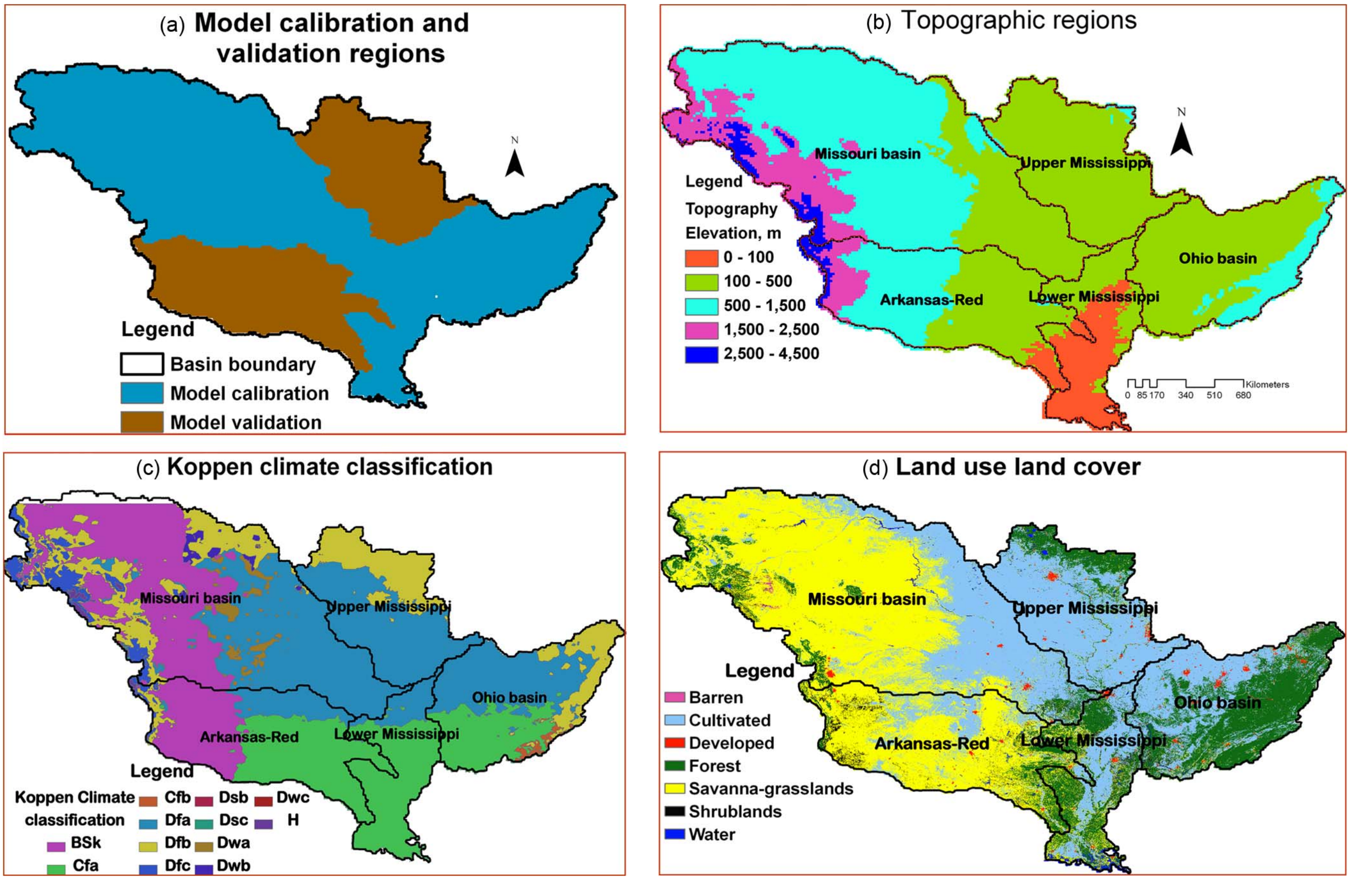

Fig. 1. Geophysical features of Mississippi River Basin (MRB). (a) Selected regions for calibration and validation of regression model framework. (b), (c) Topographic and Köppen climate regions and with five major sub-basins of MRB. (d) Land use land cover data from MODIS 2003 (*source*: http://webmap.ornl.gov/wcsdown/wcsdown.jsp?dg_id=10004_12).

and Hossain [27] studied the dependency of satellite rainfall uncertainty on topography and climate. Their study reported that the low land regions of a basin are mostly characterized by missed precipitation while the highland regions are dominated by hit bias (deviation of satellite prediction from ground observation during rainfall detection) and false precipitation. The climate of a region can also be used in segregating the nature of rainfall error attributed to a particular topographic region. For instance, in mountainous region where orographic rainfall is dominant, the rainfall rate falling within the same topographic region could significantly be different in the leeward and windward sides of the mountain. In such situations, the climate type of the region can control rainfall characteristics, which has an impact on the uncertainty of estimated satellite rainfall. Exploring the nature of satellite rainfall errors based on seasons is also essential to understand the effect of other seasonally varying meteorological and geophysical processes (such as temperature, snow cover, land use and land cover) that take place on the land surface.

Based on the above fundamental premise, a similar procedure (use of geophysical features) is adopted in the current study to estimate error variance using mathematical models. In the following sections of this paper, detail description of the study area, data and methodology are presented. Next, the results of the study are discussed. In addition, the performance of the regression model in estimating the error variance is evaluated. Finally, the finding and limitation of this work are summarized together with the future extension of the study.

II. Study Area, Data, and Methodology

The Mississippi River Basin (MRB) is chosen as the study region due to its diverse geophysical features and existence of ground truth data for validation purpose (Fig. 1). MRB has five major sub-basins: Missouri, Ohio, Lower Mississippi, Upper Mississippi, and Arkansas-Red basins. The first three basins are considered for validation purpose and the remaining two are selected for model calibration [Fig. 1(a)]. The basin is delineated into five regions based on topography features [Fig. 1(b)] to develop the regression model framework. Moreover, each region is classified according to the dominant Köppen climate type as shown on Figs. 1(c) and 2. The major land use land cover (LULC) types that inform the user about the geophysical nature of the regions are also shown on Fig. 1(d). Interestingly, the topographic regions, Köppen climate classes, and LULC somehow similar spatial patterns as shown on Fig. 1(b)–(d). Detailed description of regions is presented in Table I.

Three satellite rainfall products, namely 3B42RT, CMORPH, and PERSIANN-CCS, are used to develop error variance regression model over MRB. These satellite rainfall products are widely used, available on near-real time, and are considered fairly high resolution products for satellite-based hydrologic

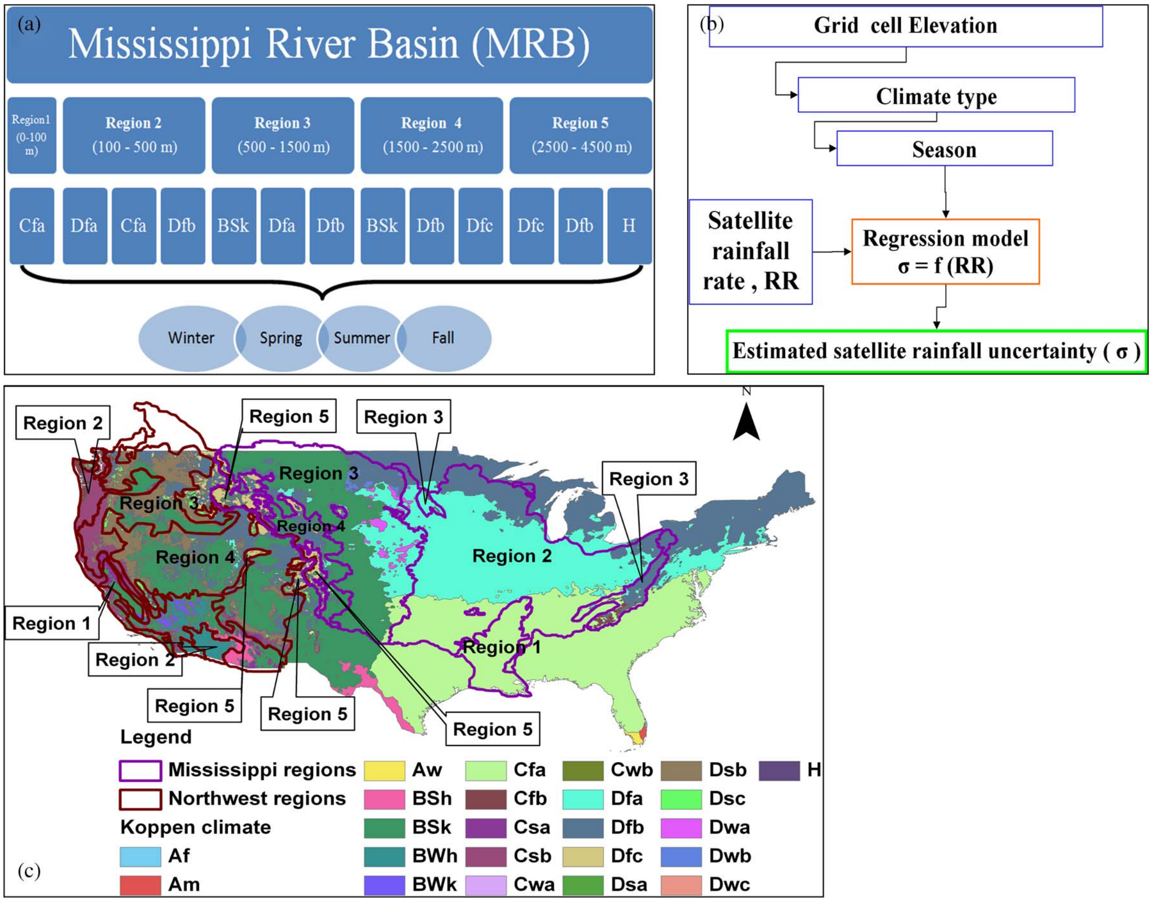

Fig. 2. (a) MRB region classification based on topography and Köppen climate type for the purpose of regression model development. The model is developed for four seasons in each region (Winter-Dec, Jan Feb; Spring-Mar, Apr, May; Summer-Jan, June, Aug; Fall-Sep, Oct, Nov). (b) Schematic representation of regression model. (c) A layer of topographic regions and Koppen climate map for MRB and Northwest Basins (NWB) to demonstrate model performance on independent basin.

application. Both 3B42RT and CMORPH, data is available at 0.25° spatial and 3 hourly temporal resolution. For the purpose of this study, the spatial resolution is downscaled to 0.125° using local scaling method [40] and the 3 hourly time scale is aggregated to a daily time step. Likewise, the PERSIANN-CCS product is aggregated to 0.125° and daily resolution from a from a 0.04° spatial and hourly resolution.

Although the focus of this study is exclusively on assessing how well error variance can be modeled mathematically regardless of scale, the choice of 0.125° as the scale of study is governed by the following factors. First, the ground truth data on rainfall is available to us at the 0.125° resolution for the CONUS region (see the detail in the next paragraph). Second, 0.125° offers a standard compromise between the PERSIANN-CCS scale of 0.04° and the typical scale of 0.25° for CMORPH and 3B42RT. Third, the aim of this study is not to compare products for their ability to be "modeled" of error variance *per se*, but rather, to assess the underlying factors of regression models and geophysical features that can assist in estimating error variance of satellite rainfall. For detail algorithm and retrieval technique of each product, readers are referred to Huffman *et al.* [5], Joyce *et al.* [6], and Hsu *et al.* [8] for 3B42RT, CMORPH, and PERSIANN-CCS, respectively.

To calibrate and validate the regression model on error variance, the observed error variance is computed using gridded ground observation rainfall data available from the Washington University's Surface Hydrology Group at the 0.125° daily scale. This data pertains to the contiguous United States (CONUS) and is derived from more than 7000 stations collected from the National Oceanic and Atmospheric Administration (NOAA) at an average density of one station per 700 km^2. The point data is gridded using synergraphic mapping system (SYMAP) interpolation algorithm [41].

A nonlinear regression model framework is developed based on the following procedure. In the first step, the MRB is grouped into five regions based on topography. Each topographic region is classified into three dominant Köppen climate classes except for region 1, which is dominated by only one type of climate class [Fig. 2(a) and (c)]. Thus, the regression model calibration is performed for 13 regions. Each of these scenarios is further broken down per season leading to $52 (= 4 \times 13)$ scenarios. Thus, to estimate the error variance over a pixel and a given day, the user first needs to have the information on topography (to classify the region it falls under), climate type and season of the day and is then guided to the appropriately calibrated regression model. In the next step, pixel's observed error variance and satellite rainfall rate are extracted for each region during the period of 2003–2006 (calibration period). The satellite rainfall rate is considered as independent (explanatory) variable; whereas the observed error variance is dependent

TABLE I
TOPOGRAPHY, KÖPPEN CLIMATE, AND LAND USE LAND COVER DESCRIPTION OF THE MISSISSIPPI RIVER BASIN

Region	Area, Km^2	Climate	%tage area	Remark	Percentage area of land use land cover						
					water	Forest	Shrub lands	Savanna-grasslands	Crop land	Developed	Barren
1	190688	Cfa	98	2% BSk, Dfa	2.7	32.0	4.5	19.2	40.2	1.2	0.3
2	1556570	Dfa	60	1% Dwa	0.2	14.2	1.4	7.5	74.9	1.7	0.0
		Cfa	28		0.6	29.5	6.2	38.9	23.9	0.9	0.0
		Dfb	11		1.5	42.4	1.0	3.3	50.8	0.6	0.2
3	1158034	BSk	50	5% Cfa, Dwa, Dwb, Cfb, Dfc	0.2	0.2	1.5	86.2	11.6	0.0	0.2
		Dfa	24		0.2	1.6	0.0	59.9	38.2	0.0	0.0
		Dfb	21		0.4	35.1	0.6	40.3	23.3	0.2	0.2
4	262140	BSk	39	5% Dfa, Dwb	0.0	1.4	3.7	91.4	2.7	0.0	0.8
		Dfb	38		0.1	11.2	2.9	78.9	5.0	1.9	0.0
		Dfc	18		0.6	35.8	3.9	53.1	6.7	0.0	0.0
5	57103	Dfc	61	6% BSk, Dsc	0.3	42.1	9.2	45.5	2.7	0.0	0.0
		Dfb	22		0.0	26.3	10.5	60.5	1.8	0.0	0.9
		H	11		0.0	30.0	20.0	46.7	1.7	0.0	1.7

Topography description
Region 1: 0 – 100 m above sea level (a.s.l)
Region 2: 100 – 500 m
Region 3: 500 – 1500 m
Region 4: 1500 – 2500 m
Region 5: 2500 – 4500 m

Land use land cover description
Forest: evergreen needle leaf, evergreen broad leaf, deciduous needle leaf, deciduous broad leaf, mixed forests
Shrub land: closed and open shrub lands
Savanna-grassland: savannas, grasslands, woody savannas
Croplands: cultivated croplands (irrigated land)
Developed: Urban and built-up
Barren: Barren or sparsely vegetated

Koppen climate description
BSk: Mid-latitude steppe - Mid-latitude dry
Cfa: Humid subtropical - Mild with no dry season, hot summer
Cfb: Marine west coast - Mild with no dry season, warm summer
Dfa: Humid continental - Humid with severe winter, no dry season, hot summer
Dfb: Humid continental - Humid with severe winter, no dry season, warm summer
Dfc: Subarctic - Severe winter, no dry season, cool summer
Dwa: Humid continental - Humid with severe, dry winter, hot summer
Dwb: Humid continental - Humid with severe, dry winter, warm summer
Dsc: Continental subarctic or Boreal climate
H: Highland climate

(response) variable. Finally, the extracted satellite data is used as input to the nonlinear regression model [Fig. 2(b)]. The method of least squares is applied to generate the estimators of the model by minimizing the sum of square error using an iterative procedure. Detailed explanation of the model calibration and optimized estimators are provided in the Appendix. Finally, the performance of the model is checked (validation) using goodness-of-fit tests (correlation, mean relative bias, and analysis of residual errors) on independent regions [Northwest basin, Fig. 2(c)] and time period (2007–2010) that were not used in calibration. The Northwest basin includes the following sub-basins: Northwest and Columbia, California, Great basin, and Colorado River basin.

Additionally, to understand the contribution of topography and climate, the regression model is developed for two scenarios: with and without geophysical feature based classification. In the first scenario, each topography and climate region has its own regression equation to predict the error variance. In the second scenario, a single regression equation is developed based on the entire calibration region without considering the topography and climate classification of the region. Ultimately, both models are tested on Northwest basin which is completely independent from the calibration region. This allowed us to elucidate the role of readily available geophysical features in improving the estimation of error variance.

III. RESULTS AND DISCUSSION

As seen on Fig. 2(b), the error variance is expressed as a function of satellite rainfall rate. It is, therefore, important to identify the spatial distribution of error component of satellite rainfall to understand its impact on error variance estimation using the regression model. On Fig. 3, 3B42RT and CMOPRH products have significant missed precipitation during the winter and summer seasons in the eastern and southern part of Mississippi basin (region 1, 2 and part of region 3). Thus, the regression model expected to underestimate or produce nil error variance in these regions.

The error variance of three satellite rainfall products is quantified at the 0.125° spatial and daily temporal scale for the period of 2003–2010. Fig. 4 presents the observed and estimated error variance spatially and seasonally averaged over topography-climate regions during the validation period (2007–2010) for 3B42RT. Generally, the magnitude of the error variance is small in region 4 and 5. This is directly related to the considerably lower rainfall intensity in these regions (Fig. 3). The observed and estimated error variances have also good agreement in these regions. However, the model underestimates the error variance in region 1-Cfa, 2-Cfa, and 2-Dfa due to the presence of missed precipitation (Fig. 3) in this region [26]. These regions are mainly dominated by cropland, forest and savanna-grassland systems.

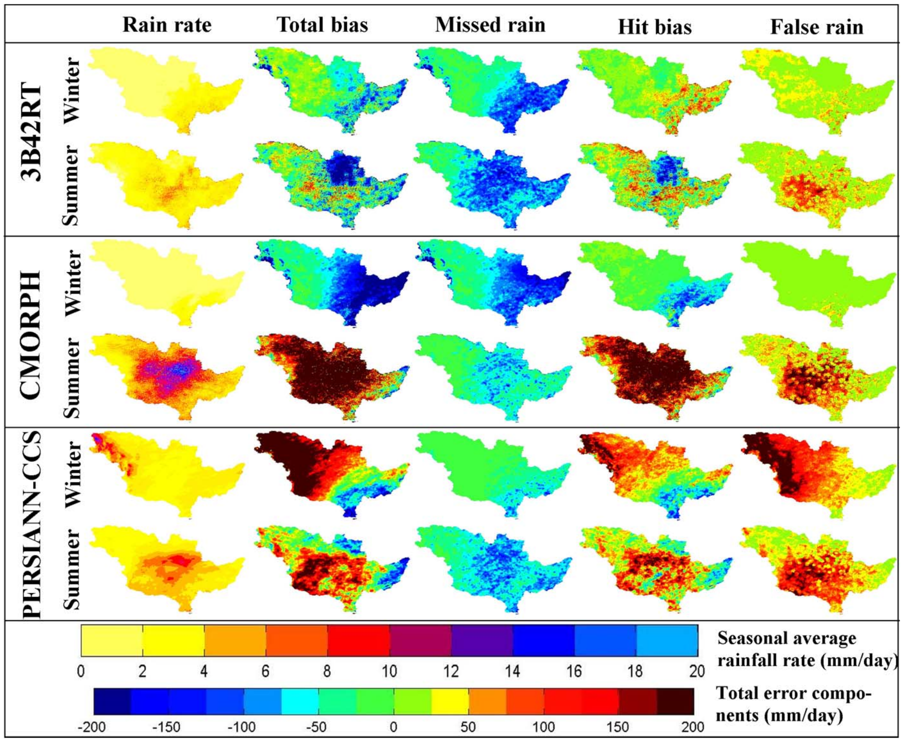

Fig. 3. Seasonal average satellite rainfall rate and the total error components (total bias, missed-rain bias, hit bias, false-rain bias) for the winter and summer seasons.

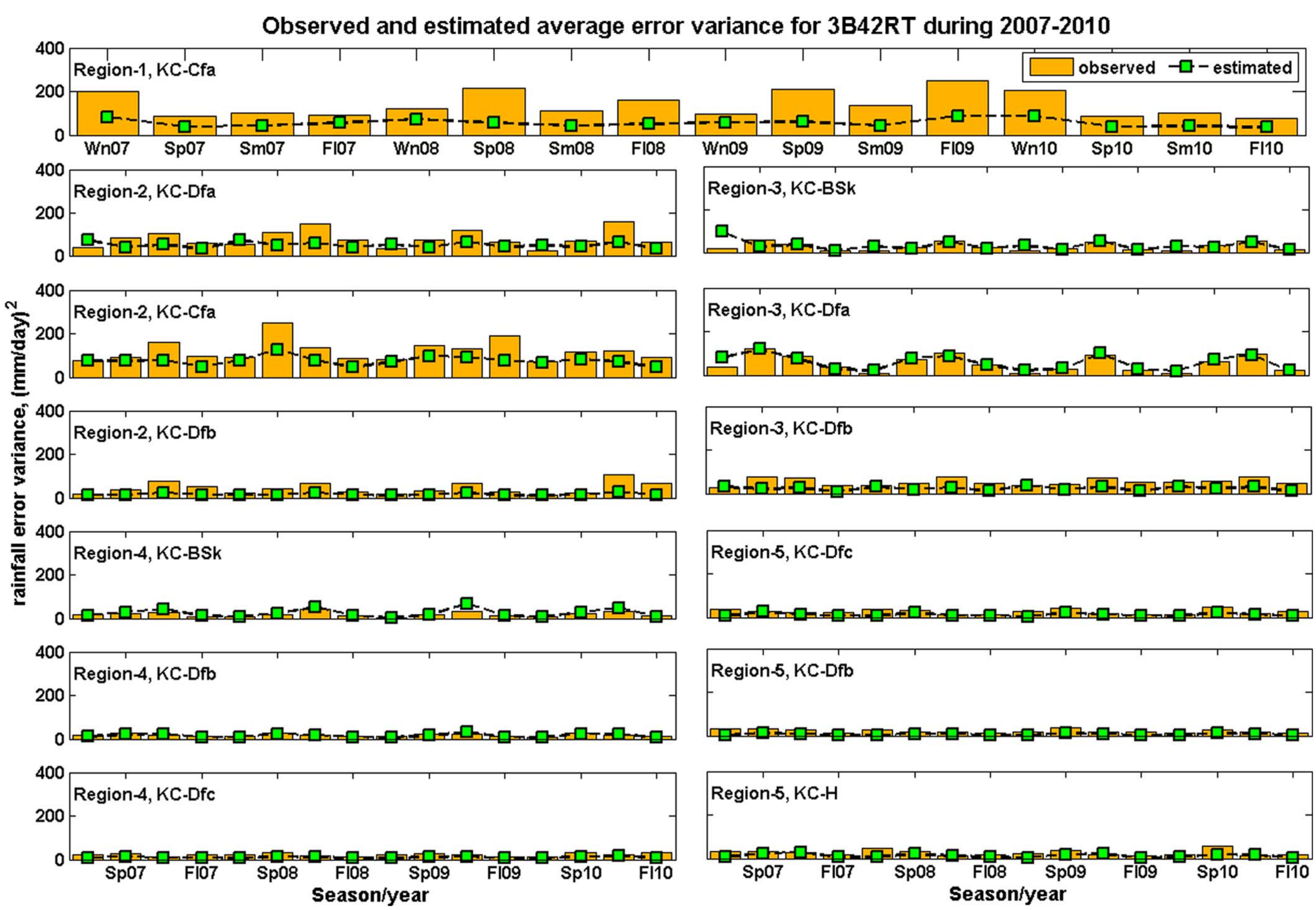

Fig. 4. Estimated and observed error variance for 3B42RT satellite rainfall product, spatially and seasonally averaged over topographic and Köppen climate regions of MRB for the validation period (2007–2010). Region code is based on Table I. (Wn: winter; Sp: spring; Sm: summer; Fl: fall seasons).

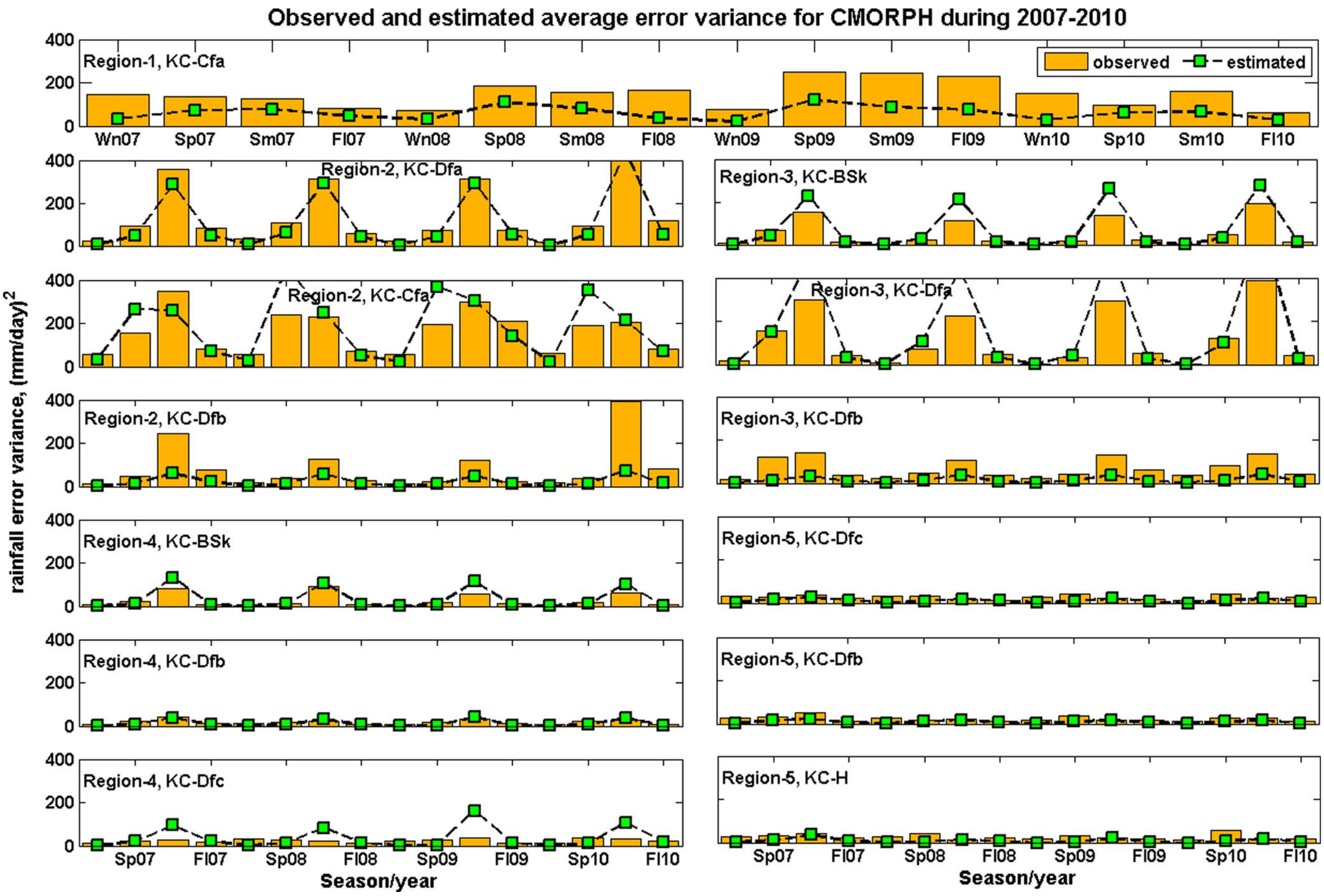

Fig. 5. Same as Fig. 4, except for CMOPRH rainfall product.

As seen in Fig. 5, the estimated error variance from CMORPH is also underestimated in regions 1-Cfa, 2-Dfb, and 3-Dfb, mostly as a result of missed precipitation (Fig. 3). These regions are mostly characterized by forest, cropland and savanna-grassland system. But the model slightly overestimates in regions 3-BSk and 3-Dfa (both regions are dominated by savanna-grassland system) due to the existence of positive hit bias for CMORPH product, reported earlier by Gebregiorgis *et al.* [26] or refer to Fig. 3. On Fig. 6, the error variance estimated from PERSIANN-CCS is relatively more accurate for regions 1 and 2. But in regions 3-BSk, 3-Dfa, and 4-BSk, this product over predicts the error variance especially during the winter and spring seasons. In regions 4-Dfb, 4-Dfc, and 5-H, it overestimates the error variance during winter season. These regions are also mostly covered by savanna-grassland systems. This is mainly caused by false precipitation and positive hit bias during the cold seasons (Fig. 3). In general, the above results reveal that the regression model performs well and captures the trend of observed error variance in the region where hit bias and false precipitation are dominant components of the error. However, if the region is dominated by missed precipitation, the model's predictability is compromised because of the satellite data reporting extensive zero rainfall rates. This is one of the main limitations of the power-law type multiplicative type error model used in the study (discussed later).

Fig. 7–9 present the time series of error variance spatially averaged over the major Mississippi sub-basins (calibration and validation regions) for the entire period of simulation (2003–2010). A 31-day moving average is applied to the time series data (observed and estimated error variances) to reduce visual cluttering. In case of 3B42RT product, the trends of the observed and estimated error variance are closely similar in Missouri basin during the entire period (Fig. 7). This is not true, however, for Lower Mississippi, Ohio, Upper Mississippi, and Arkansas-Red basins. The model fails to capture the peaks of observed error variance, particularly during the cold seasons. On the other hand, in case of CMORPH product (Fig. 8), the model displays outstanding performance for all sub-basins during the entire period of validation. For PERSIANN-CCS, the drift of observed and estimated error variances in all sub-basins is qualitatively similar (Fig. 9). However, the model overestimates the error variance in Missouri basin almost during the entire period due to the inherent problem of false precipitation in PERSIANN-CCS as reported earlier by Gebregiorgis *et al.* [26] (also see Fig. 3). In general, this reinforces that the main type of error component (hit, miss or false precipitation) that is associated with a particular product directly affects the performance of the regression model at a given location.

The residual error variance (which is defined in this case, as the difference between estimated and observer error variance), computed over the entire basin, is shown on Fig. 10. Residuals

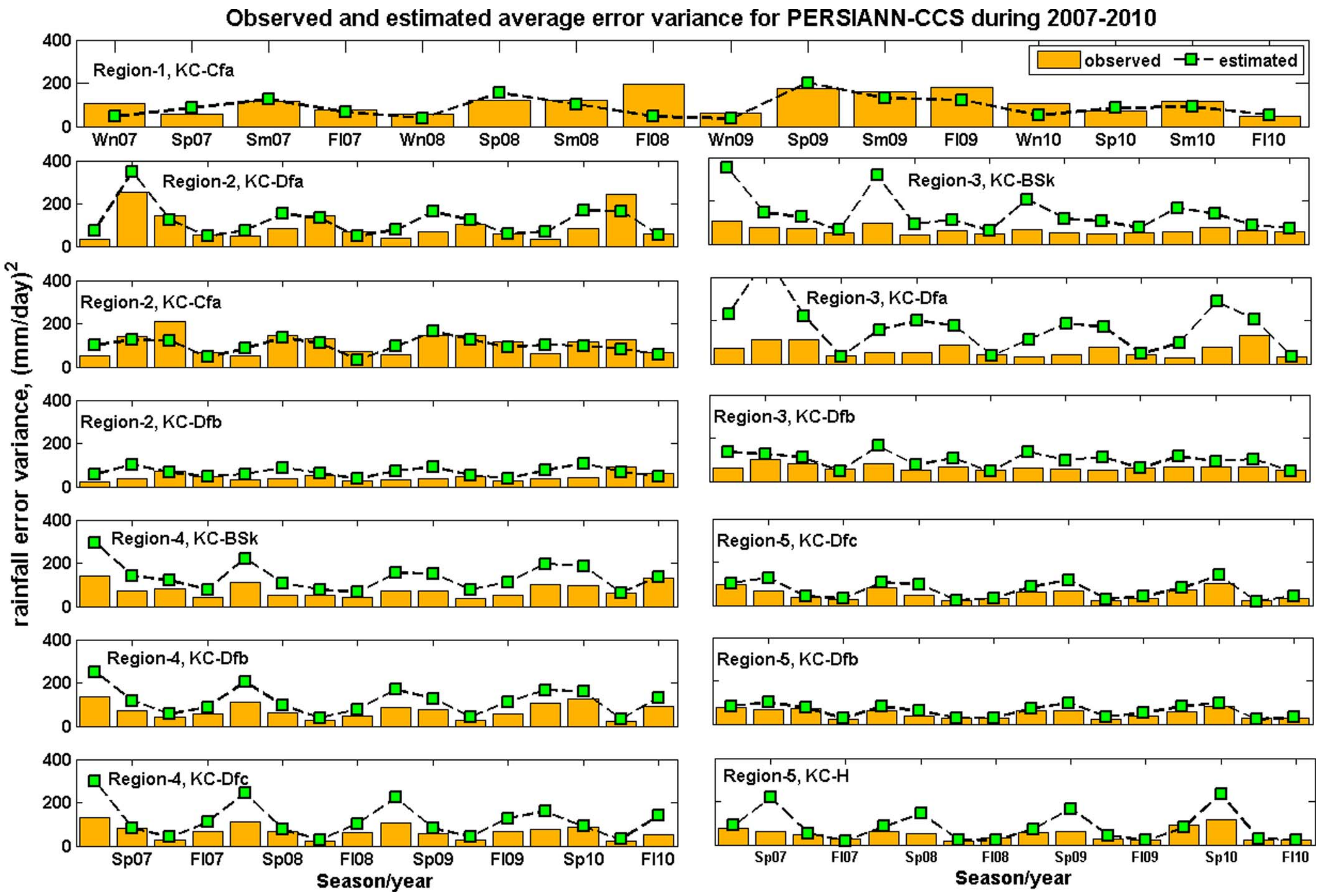

Fig. 6. Same as Fig. 4, except for PERSIANN-CCS rainfall product.

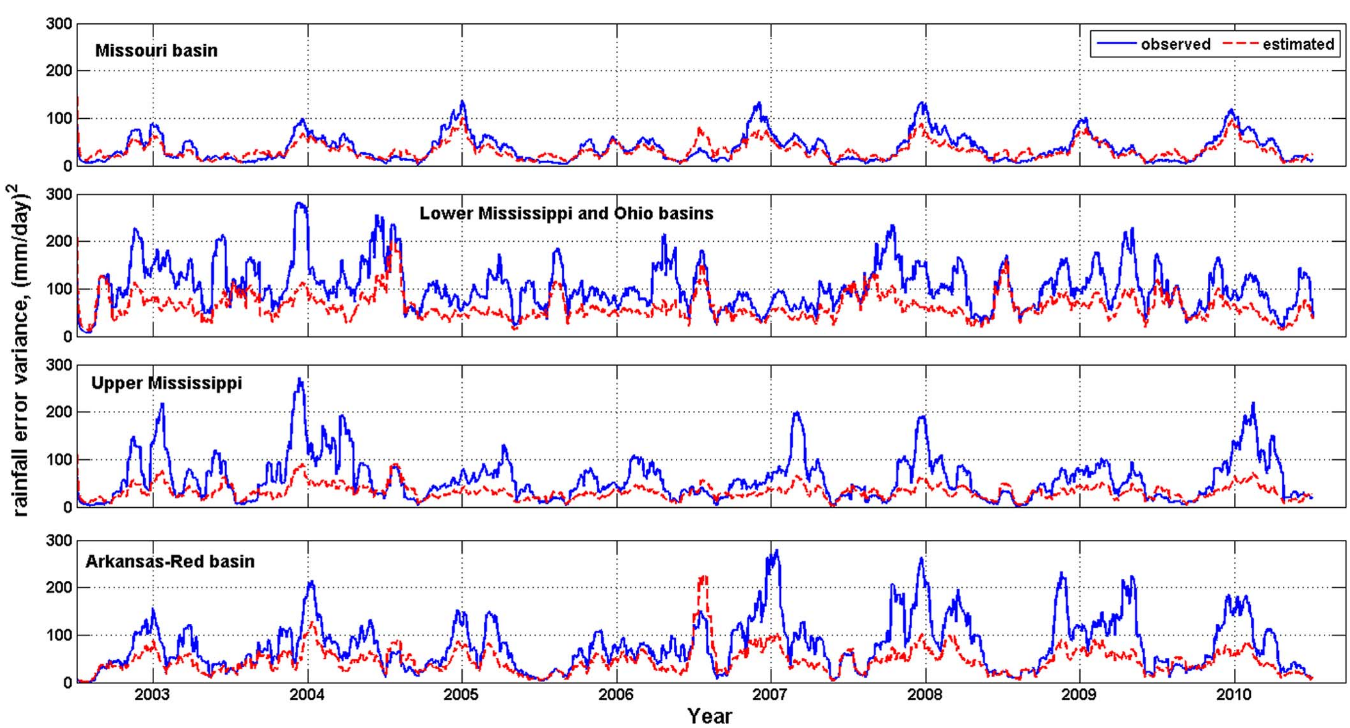

Fig. 7. Estimated and observed daily time series of error variance for 3B42RT rainfall product, spatially averaged over the selected calibration (top two panels) and validation sub-basins (bottom two panels) during the period of 2003–2010. A 31-day moving average is applied to reduce visual cluttering.

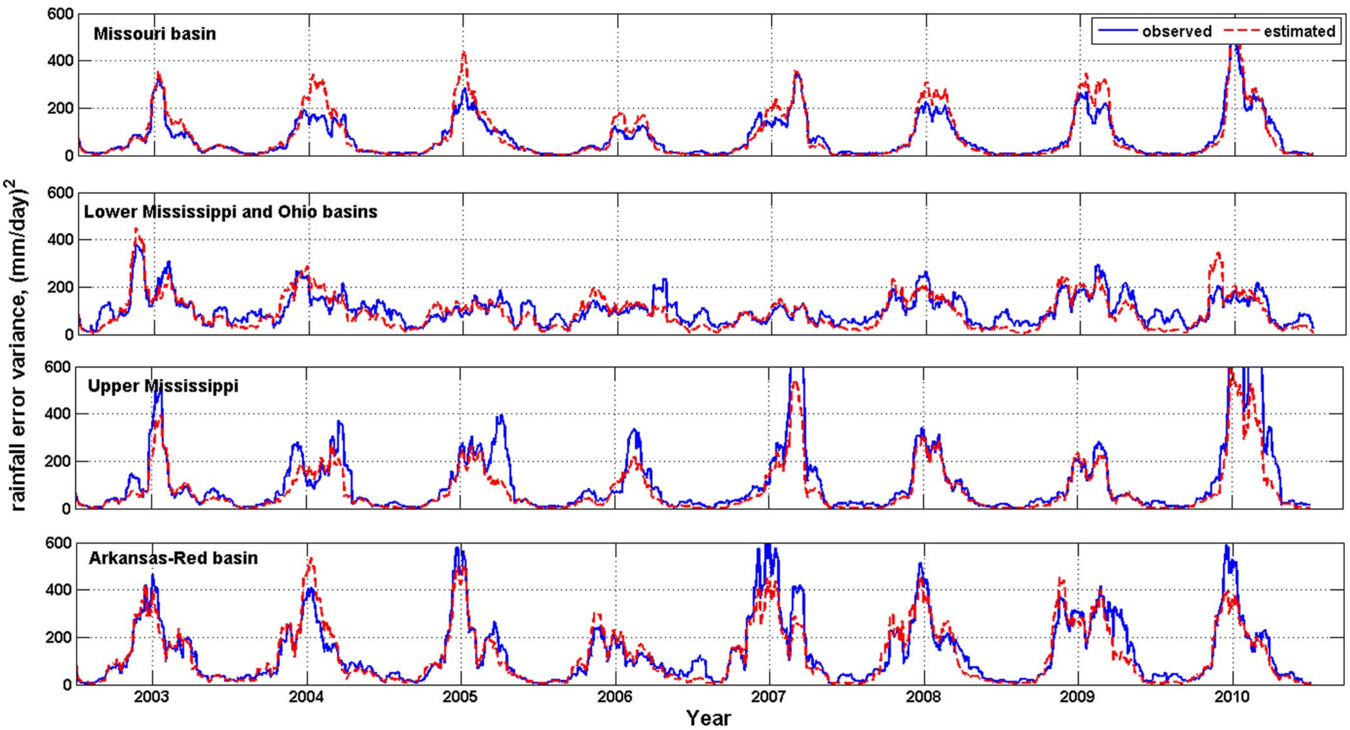

Fig. 8. Same as Fig. 7, except for CMORPH rainfall product.

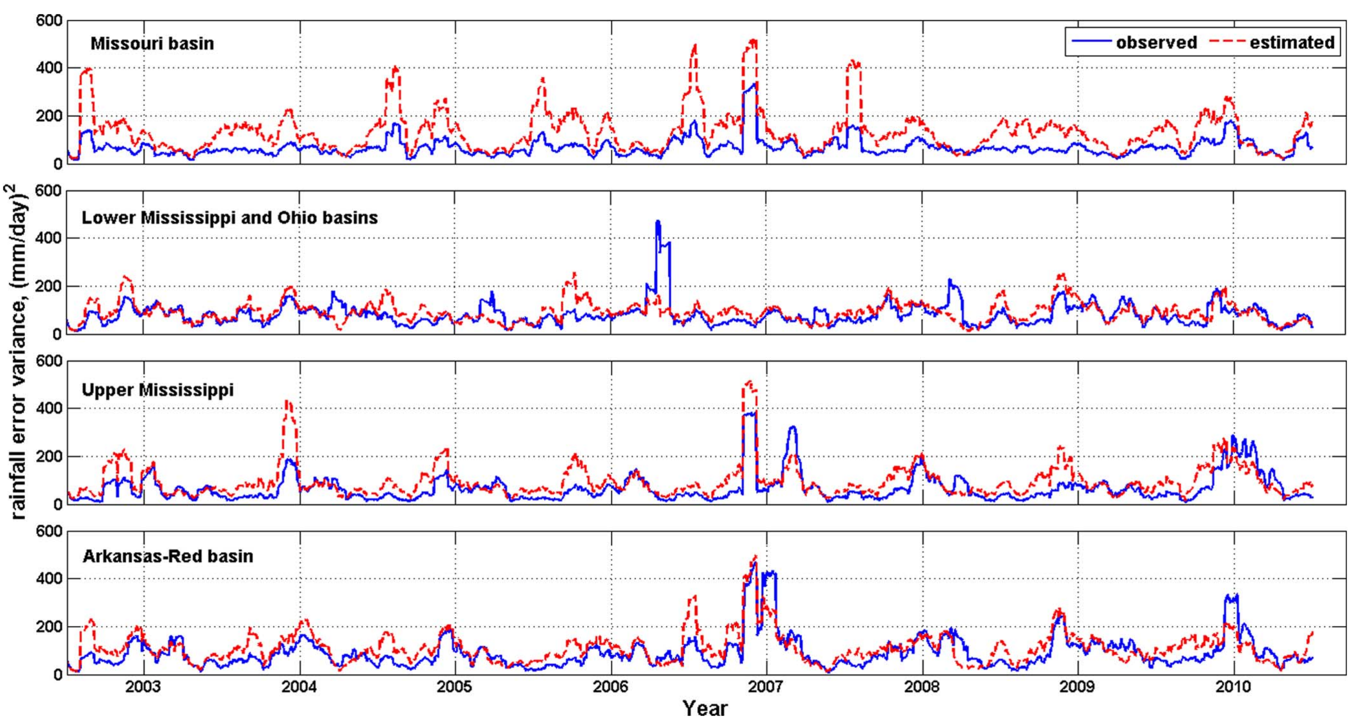

Fig. 9. Same as Fig. 7, except for PERSIANN-CCS rainfall product.

provide a general idea of the required unbiased nature of a predictive model. In general, the modeling approach seems to be relatively unbiased for all satellite rainfall products during the independent validation period (2007–2010). It captures the spatial pattern of the observed error variance. The unbiased regions mostly show non-zero actual rainfall records (ratio of error variance to ground rainfall (EV/GR) is greater than zero). The estimated error variance shows quantitative offset from the observed in range of -400 to 400 $(\text{mm/day})^2$ (or -20 to 20 mm/day in standard deviation). As expected, 3B42RT is a little skewed toward negative residual error variance because of more missed rain.

Fig. 11 shows the comparison of spatially and seasonally averaged observed and estimated error variance over the developed topography-climate regions and seasons. In case of all products, the estimated and observed error variances are reasonably comparable. In case of 3B42RT, the computed mean error variance in region 1-Cfa is underestimated during winter

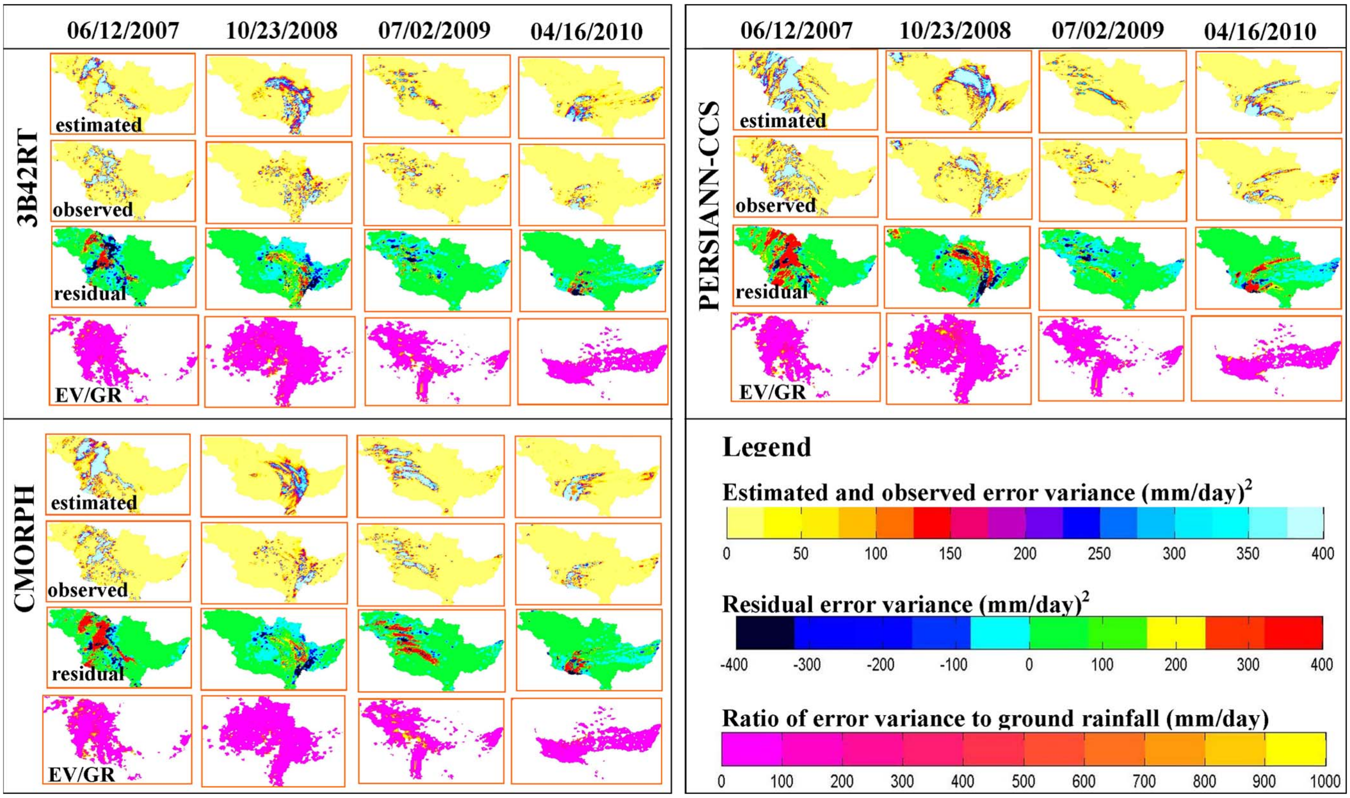

Fig. 10. Estimated, observed, and residual error variance and ratio of computed error variance to ground rainfall value for three satellite rainfall products over the MRB for four randomly selected days during the validation period (2007–2010). (EV: error variance; GR: ground rainfall).

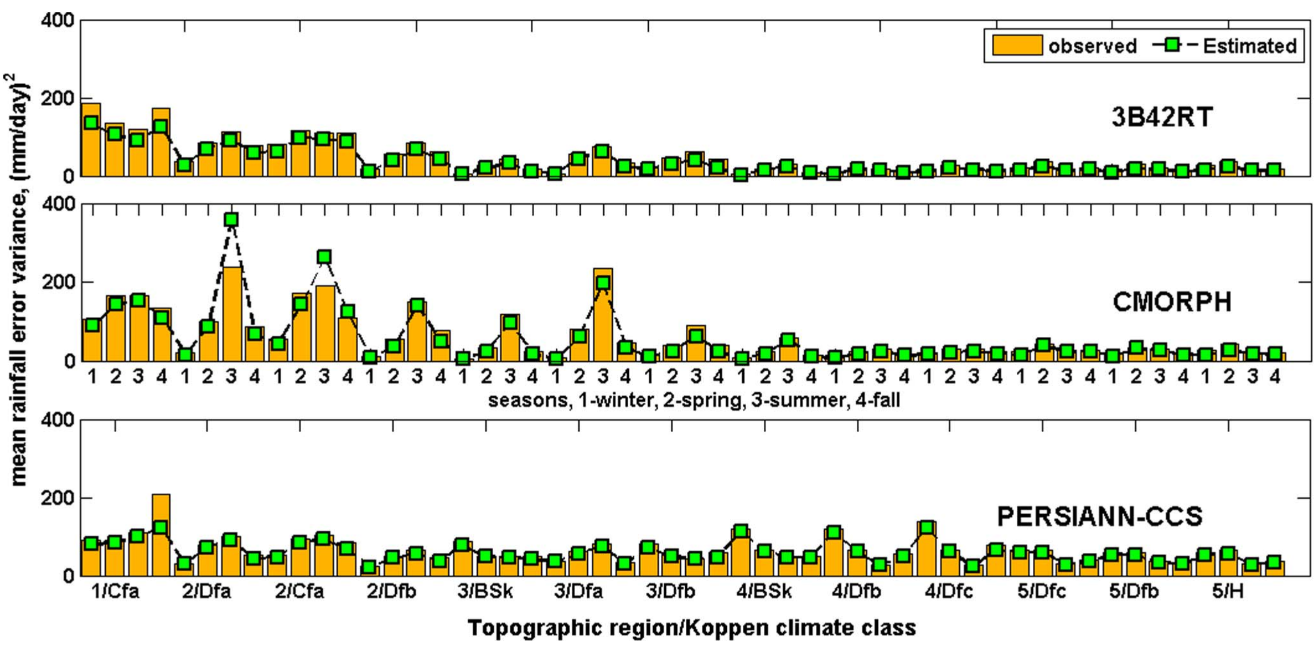

Fig. 11. Mean observed and estimated error variance of satellite rainfall products during the calibration period (2003–2006) for the 13 topographic and climate regions and 4 different seasons. The x-axis on the lower panel shows the topographic region and climate types, and on the middle panel it displays the seasons for each region.

and fall seasons; for CMORPH, the estimated error variance is larger than the observed in region 2-Dfa and 2-Cfa during the summer season; and for PERSIANN-CCS, the predicted mean variance is underestimated only in region 1-Cfa during fall season. In general, the model shows good performance for CMORPH and PERSIANN-CCS products.

To understand the proportion of variance of the dependent variable (error variance) explained by the independent variable (rainfall rate), the following parameters are computed: the total variance of the dependent variable (total sum of squares, TSS), the proportion of variance due to the residuals (error sum of squares, SSE), and the proportion of variance due to the

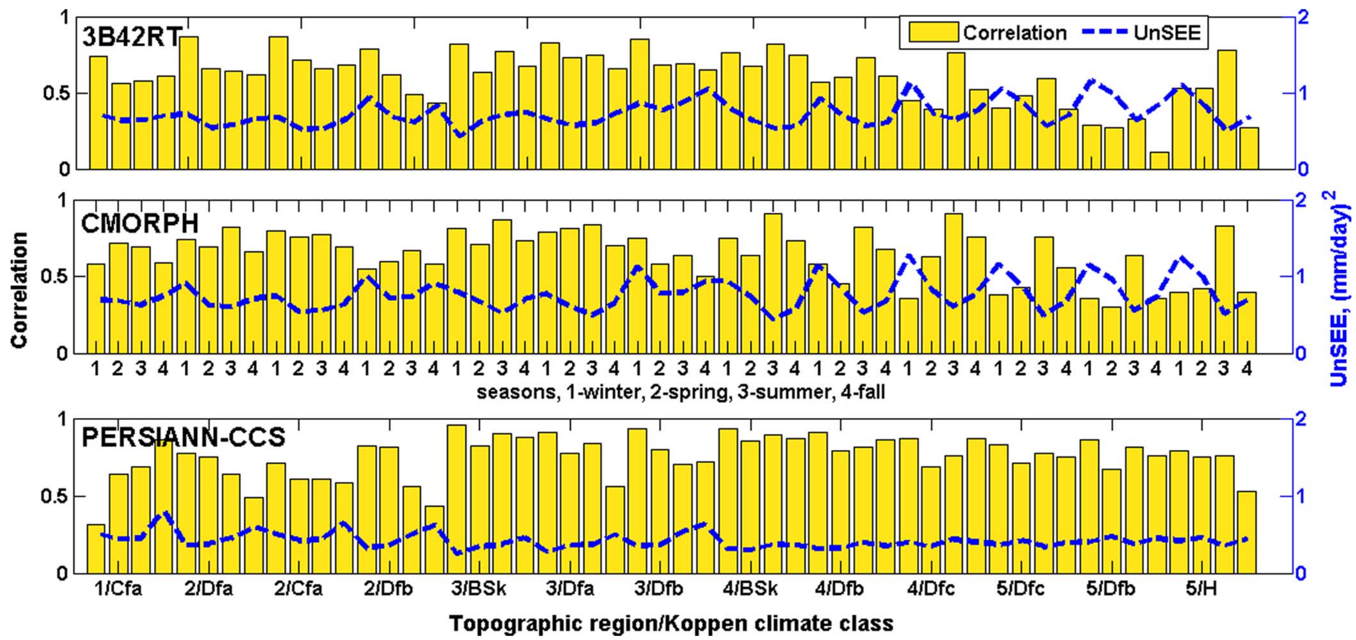

Fig. 12. Ratio of SSR/TSS (correlation) and unbiased standard error of estimate (UnSEE) of observed and estimated error variance of satellite rainfall products during the calibration period (2003–2006) for the 13 topographic and climate regions and 4 different seasons.

regression model (regression sum of squares, SSR = TSS-SSE). The ratio of the regression sum of squares to the total sum of squares (SSR/TSS) explains the proportion of variance accounted for in the dependent variable (error variance) by the model, in other words, it shows the correlation between the observed and predicted error variance. Fig. 12 presents the correlation (SSR/TSS) of the observed and estimated error variance. In general, for most of the regions and products, the ratios of SSR/TSS are generally larger than 0.5. However, it shows distinct features among product types and also regions. For 3B42RT and CMORPH products, the correlation reduces from lowland to highland regions. For both products, during winter, the correlation is significantly very low. For PERSIANN-CCS products, the SSR/TSS ratio increases from lowland to highland regions.

The standard error of estimate (SEE) is another measure of the accuracy of predictions which is the squared root of the average squared deviation. To make the sample standard error of estimate an unbiased estimator for the population, the degrees of freedom in the denominator of the estimator is modified as N-2 and the adjusted SEE is called unbiased standard error of estimate (UnSEE). The smaller the standard error of the estimate is, the more accurate the predictions are. Fig. 12 also presents the UnSEE of the observed and estimated error variance. In general, the PERSIANN-CCS has the smallest SEE as compared to the other two products.

The mean relative bias (MBias) also measures the agreement between observed and estimated error variance. The allowable limit for MBias is between -40% and 40% with zero as the ideal value [42]. Table II illustrates the correlation coefficient (SSR/TSS) and mean relative bias (MBias) based on sub basins. Accordingly, the model predicts the error variance very well over Missouri, Lower Mississippi and Ohio basins using CMORPH and PERSIANN-CCS products; whereas the prediction obtained from 3B42RT and CMORPH is more accurate over Upper Mississippi.

TABLE II
CORRELATION COEFFICIENT (SSR/TSS) AND MEAN RELATIVE BIAS (MBIAS,%) OF OBSERVED AND ESTIMATED ERROR VARIANCE BY SUB-BASINS

Sub-basin name	3B42RT		CMORPH		PERSIANN	
	SSR/TSS	MBias	SSR/TSS	MBias	SSR/TSS	MBias
Missouri	0.63	46.0	0.83	14.4	0.80	-10.0
Lower Mississippi and Ohio basins	0.80	36.3	0.74	12.0	0.63	-15.4
Upper Mississippi	0.75	15.9	0.86	-3.8	0.87	-46.8
Arkansas-Red basins	0.59	45.6	0.89	35.9	0.92	-32.1
Northwest basin *	0.85	-34.0	0.48	17.0	0.60	-37.0
Northwest basin **	0.63	66.0	0.44	-53.0	0.51	83.0

* With geophysical feature based classification

** Without geophysical feature based classification

To look further into the performance of the regression model, the error variance has been estimated for Northwest basin. Fig. 13 presents the spatial error variance distribution of the three satellite rainfall products for the four seasons over the Northwest basin. In this case, the regression model that considers geophysical features is implemented. For 3B42RT (Fig. 13 top three panels), the model captured the spatial distribution pattern adequately over entire region despite quantitative accuracy of prediction. The model performance for CMORPH (Fig. 13 middle three panels) is similarly good except it has underestimated the error variance during the winter season. As

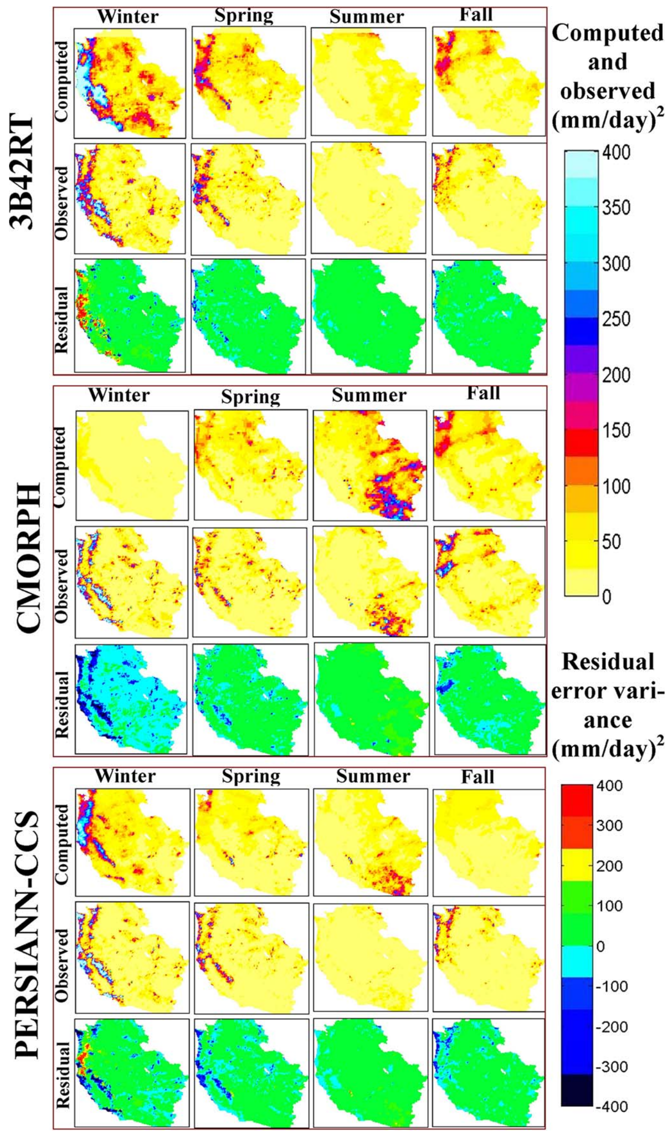

Fig. 13. Computed, observed, and residual seasonal average error variance for three satellite rainfall products over the NWB for the period of 2004–2005. The regression model is developed based on geophysical regions (topography and Koppen climate).

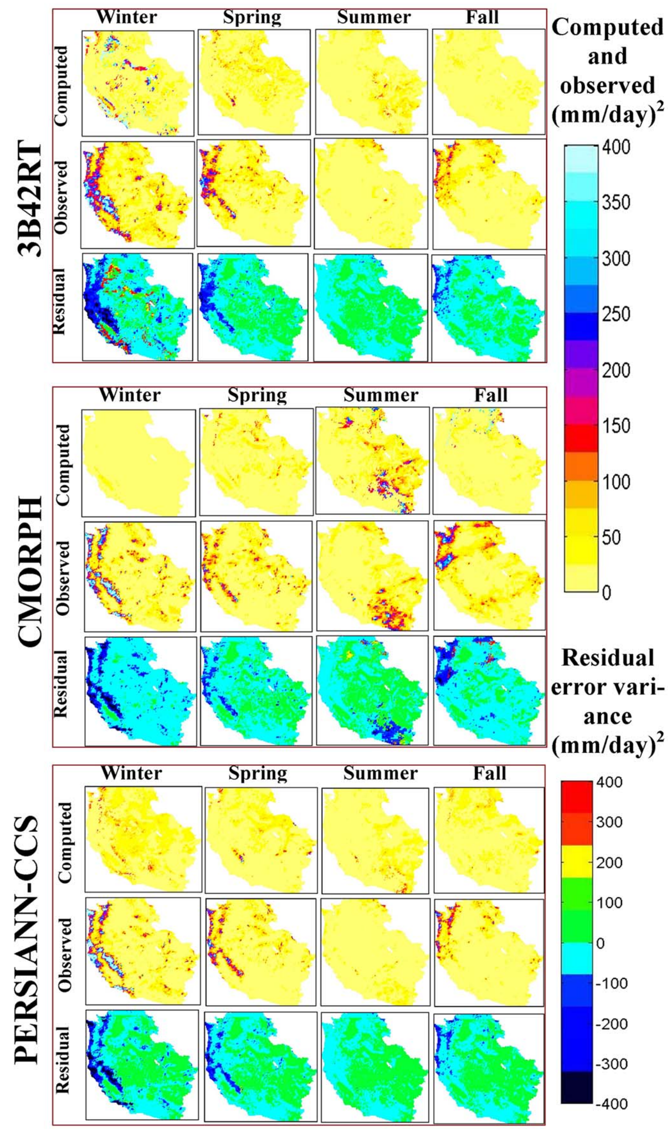

Fig. 14. Same as Fig. 13, except the regression model is developed without the consideration of geophysical features.

it has been discussed earlier for MRB case, the underestimation is possibly due to missed precipitation particularly over Pacific coastal region. The estimated error variance for PERSIANN-CCS (Fig. 13 bottom three panels) is somehow different from the observed error variance during spring, summer and fall seasons. It has tendency to overestimate on some part of the region and underestimate elsewhere.

Fig. 14 shows the comparison of observed and computed error variance using the regression model that does not consider geophysical features. The model does not capture the spatial pattern of the observed error variance for all satellite products. This shows that the geophysical features play an important role in the error variance estimation. The trend of temporal error variance over the Northwest basin for both scenarios is presented on Fig. 15. From qualitative comparison, there is no significant difference in the model performance except that the CMOPRH and PERSIANN-CCS over predict the error variance during the summer season. Table II also presents the SSR/TSS and MBias of the estimated and observed error variance for Northwest basin. The regression model based on classification of geophysical feature demonstrates good performance as compared to without region classification. The former scenario shows that the SSR/TSS is 0.85, 0.48, and 0.60 for 3B42RT, CMORPH, and PERSIANN-CCS, respectively. Without the classification of geophysical feature, the SSR/TSS is 0.63, 0.44, and 0.51 for the respective rainfall products.

One of the limitations for independently testing the regression model is that some of the climate types in Northwest basin are not available in MRB. Therefore, matching of closely similar climate type was made in error variance estimation procedure. The Koppen climate classes specific to Northwest basin (NWB) includes BWh (dry subtropical desert), BSh (dry subtropical steppe), Csa (Mild mid-latitude with dry, hot summer), Csb (Mild mid-latitude with dry, warm summer), and Dsb (Sever mid-latitude continental with warm summer). For instance, the dominant climate class in region 2 of NWB Csb

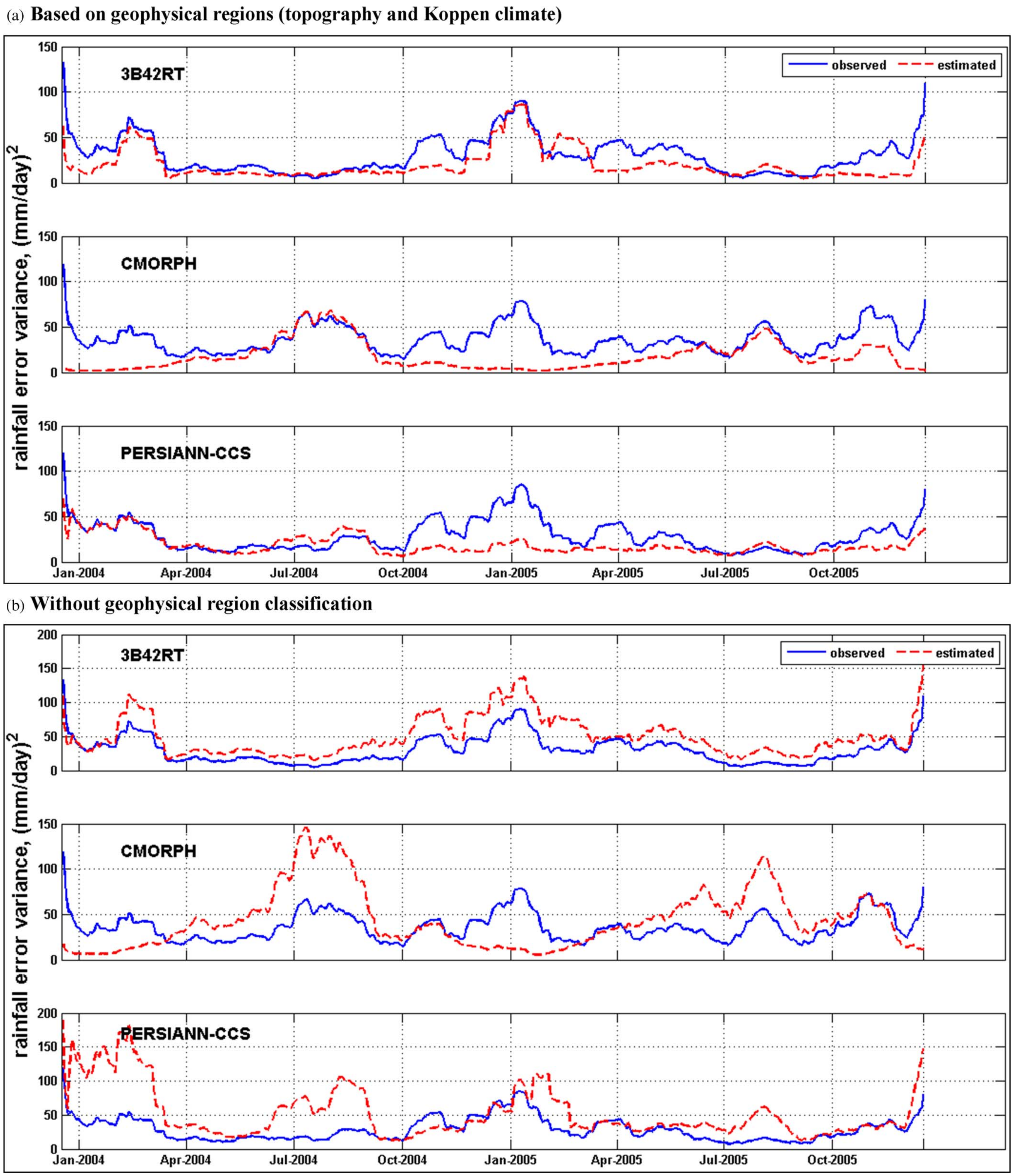

Fig. 15. Estimated and observed daily time series of error variance spatially averaged over NWB for the period of 2004–2005 using the regression model developed with and without geophysical region classification (upper and lower panels, respectively). A 31-day moving average is applied.

is matched with Cfa of MRB; Dsa in region 4 of NWB with Dfb of MRB and so on. Such a "mapping" could affect the estimation of error variance. Therefore, it is recommended to develop the regression model on a large-scale basin where the entire spectrum of the diverse geophysical features is existent.

IV. Conclusion and Recommendation

As satellite rainfall estimates become more important for hydrologic and atmospheric applications, users' knowledge on uncertainty associated with the satellite rainfall product is a

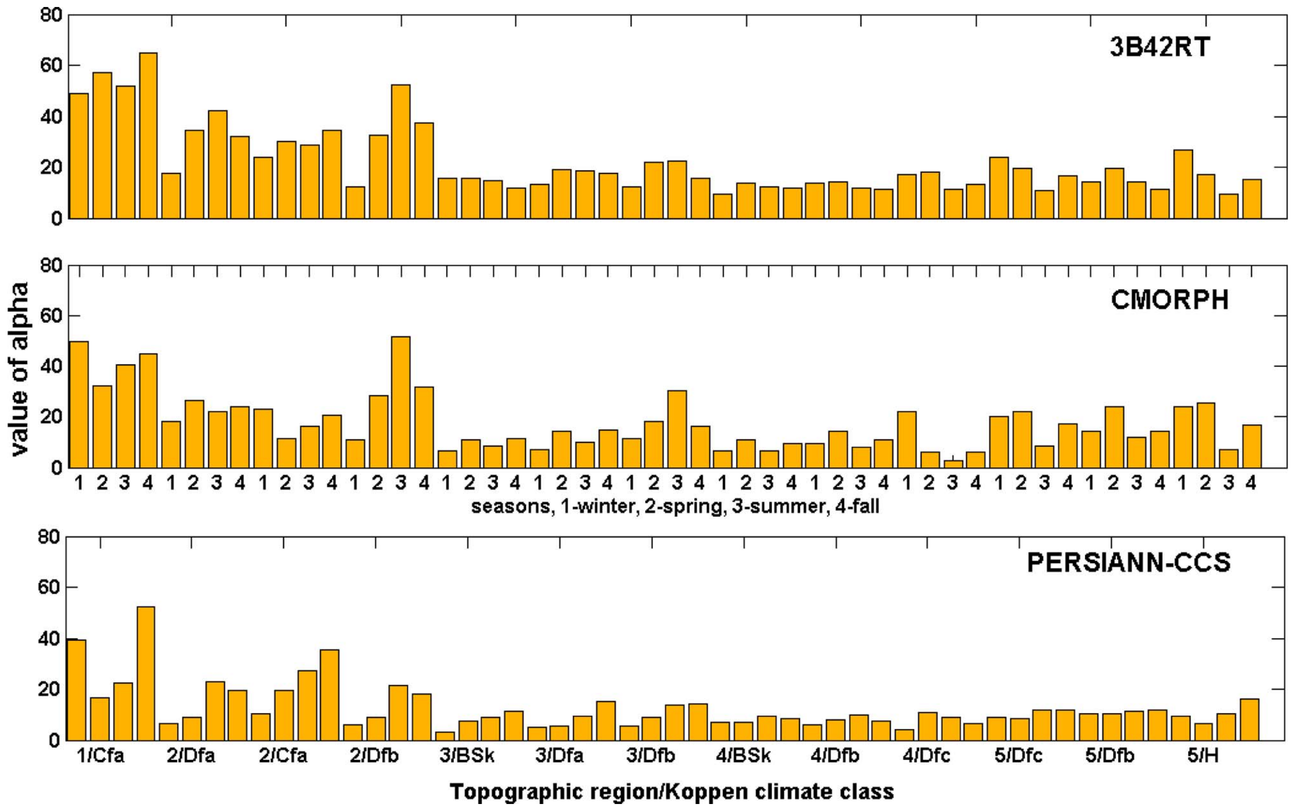

Fig. 16. Computed value of scaling factor (α) for different regions of MRB for the three satellite rainfall products.

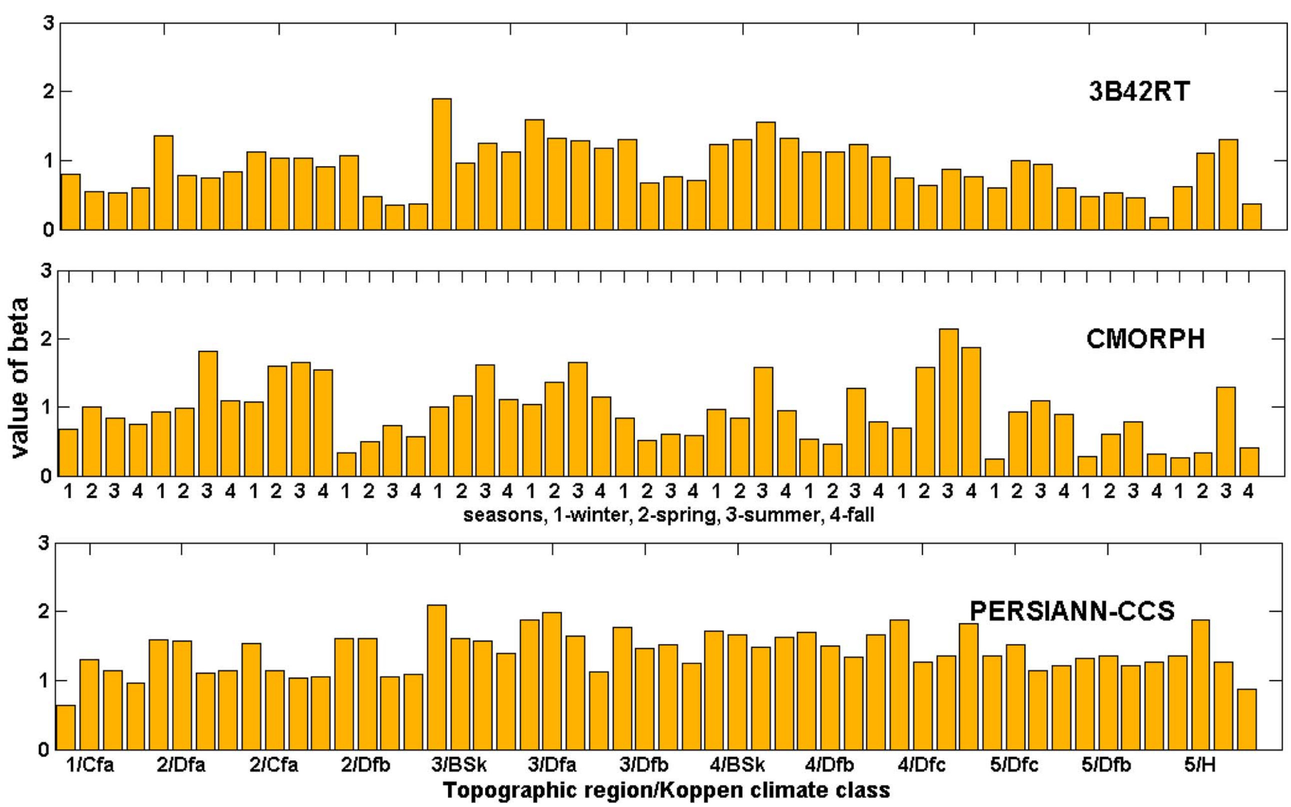

Fig. 17. Computed value of power or exponent (β) for different regions of MRB for the three satellite rainfall products.

necessary step to advance its application. A simple nonlinear regression model has been developed for 3B42T, CMORPH, and PERSIANN-CCS products to estimate the error variance at the 0.125° spatial and daily temporal resolution. Topography, climate and seasons are considered as readily available geophysical features for enhancing the predictive ability of the model at any location. In general, topography plays a direct role on the pattern of climate of the region due to its forcing on the formation of clouds, temperature and albedo. These climatic and weather-scale processes strongly influence the effectiveness of indirect approach of the remote sensing measurement technique. Therefore, use of topography, climate and season as major governing factors in the development of regression framework is logical to identify the uncertainty type associated with satellite rainfall estimates.

The findings of this study can be summarized into the following three major points.

1) The error variance (EV) has a strong correlation and is directly proportional to the rainfall rate (RR). The relation between the two variables can be adequately expressed by a power function $\mathrm{EV} = \alpha(\mathrm{RR})^{\beta}$, where α and β are constant real numbers. The parameter "α" serves as simple *scaling factor*, moving the values of "$(\mathrm{RR})^{\beta}$" up or down as the value of "α" increases or decreases, respectively. The parameter "β" is called the exponent or power that determines the rate of growth or decay and also shape and behavior of the function.
2) In general, the parameter "α" is high for 3B42RT, moderate for CMORPH, and small for PERSIANN-CCS products (see Fig. 16). For all products, "α" gradually decreases from lowland to highland regions. The value of "β" is found to be high for PERSIANN-CCS product and there is no significant variation among different regions. For 3B42RT and CMORPH, "β" shows considerable variation from season to season without obvious systematic trend across the regions (see Fig. 17).
3) The type of error components (missed rain, hit, and false-rain biases) that is present in the satellite rainfall estimates has a direct impact on the performance of regression model. The model estimates the error variance more accurately when hit or false precipitation is dominant in the product. On the other hand, the presence of large missed precipitation, makes a product less amenable for error variance estimation.

The key limitation of this study is the model's inability to predict the error variance accurately in a region where missed precipitation is dominant. If satellite product predicts zero rainfall, then the estimated error variance will be zero by design. Therefore, further exploration is needed to know the location where missed rain is more likely to occur and include other independent (additive) variables in the regression model to estimate the error variance in such conditions. Moreover, the proposed method has a conceptual limitation when the precipitation errors depend heavily on other factors such as physical properties of rain systems. Further exploration on these issues will help improve the concept of this study for practical applications.

On the basis of the promising results reported herein, further investigation into the impact of diverse geophysical features on the performance of regression model by extending the study region to a global scale is now appropriate. Future investigation should also target the quantification of the probabilistic behavior of missed rain as a function of terrain, climate and satellite rain rate. Such an assessment may allow proxy adjustments to avoid the aforementioned limitation of zero error variance prediction.

In summary, high resolution and multisensor satellite-based precipitation estimates, such as those analyzed in this study and those anticipated from the Global Precipitation Measurement (GPM; http://gpm.gsfc.nasa.gov) satellites, now hold great promise for hydrologic applications, especially over parts of the world where surface observation networks are sparse, declining or non-existent. However, the usefulness of such precipitation products for hydrological applications will depend on their error characteristics and how successful we are in intelligently harnessing the implications of uncertainty for surface hydrology. The decline of the few existing global ground based measurement networks for rain and stream flow and the absence of *in-situ* measurement in most parts of the world represent a "paradoxical" situation for evaluating satellite rainfall estimation uncertainty. By developing simple models for estimation of error variance for satellite data that a user can use *anywhere* and *anytime* using only readily available geophysical features, our study represents a first comprehensive step at resolving the paradox for the GPM era.

Appendix A
Mathematical Formulation of Regression Model

Regression is a highly useful statistical method for developing a quantitative relationship between dependent variable and one or more independent variables. The dependent variable often is called response or predicted variable. The independent variables that explain the response variable are called explanatory or predictor variables. In this paper, the dependent variable is defined as error variance, EV and the independent variable is satellite rainfall rate, RR.

The proposed nonlinear functional relation between the two variables is expressed as

$$EV = \alpha(RR)^{\beta} \tag{A1}$$

where, α and β are constant real number and are called scaling factor and power, respectively. The nonlinear equation can be converted to linear equation by applying logarithmic function in (A1)

$$\log(\mathrm{EV}) = \log(\alpha) + \beta\log(\mathrm{RR}). \tag{A2}$$

Let $y = \log(\mathrm{EV})$, $\alpha_{\mathrm{o}} = \log(\alpha)$, $\alpha_1 = \beta$, and $x = \log(\mathrm{RR})$, then (A2) can be written as form of linear regression form.

$$y = \alpha_{\mathrm{o}} + \alpha_1 x. \tag{A3}$$

For i^{th} observation, the predicted value can be written as:

$$Y_{\mathrm{i}} = \alpha_{\mathrm{o}} + \alpha_1 x_{\mathrm{i}}.$$

If $\mathrm{EV_o}$ is the observed error variance then the logarithmic form of the observed error variance for the I^{th} observation, y_{oi}

$$y_{\mathrm{oi}} = \log(\mathrm{EV_o}).$$

Applying least square method (LSM) to minimize the error sum of the squares (SSE) $SSE = \sum_{i=1}^{n}(y_{oi} - y_i)^2$ for n number of observation

$$SSE = \sum_{i=1}^{n}(y_{oi} - \alpha_o - \alpha_1 x_i)^2. \tag{A4}$$

To minimize the sum of error square differential (A4) and equate to zero

$$\frac{\partial(SSE)}{\partial\alpha_o} = \frac{\partial}{\partial\alpha_o}\left(\sum_{i=1}^{n}(y_{oi} - \alpha_o - \alpha_1 x_i)^2\right) = 0 \tag{A5}$$

$$\frac{\partial(SSE)}{\partial\alpha_1} = \frac{\partial}{\partial\alpha_1}\left(\sum_{i=1}^{n}(y_{oi} - \alpha_o - \alpha_1 x_i)^2\right) = 0. \tag{A6}$$

Equations (A5) and (A6) are called normal equations. Carrying out the differentiation, we obtain

$$n\alpha_o + \alpha_1 \sum x_i = \sum y_{oi}$$

$$\alpha_o \sum x_i + \alpha_1 \sum x_i^2 = \sum y_{oi} x_i$$

where all the summation go from $i = 1$ to $i = n$. The solution to these normal equations can be given as

$$\alpha_o = \overline{y_o} - \alpha_1 \overline{x} \quad \text{and}$$

$$\alpha_1 = \frac{\sum_{i=1}^{n}(x_i - \overline{x})(y_{oi} - \overline{y_o})}{\sum_{i=1}^{n}(x_i - \overline{x})^2}.$$

Finally, convert the logarithmic scale back to normal

$$\alpha = \text{anti} - \log(\alpha_\text{o})$$

$$\beta = \alpha_1.$$

For 3B42RT, CMORPH, and PERSIANN-CCS products, the value of α and β are computed for the developed topography-climate regions as shown in Figs. 16 and 17, respectively.

Acknowledgment

The authors are grateful to the hydrology research group at the University of Washington for providing ground rainfall data. The authors also acknowledge the technical support received from M. Renfro of the Computer-Aided Laboratory at the Center for Manufacturing Research, Tennessee Technological University.

References

[1] G. J. Huffman, R. F. Adler, B. Rudolf, U. Schneider, and P. R. Keehn, "Global precipitation estimates based on a technique for combining satellite-based estimates, rain gauge analysis, and NWP model precipitation information," *J. Climate*, vol. 8, no. 5, pp. 1284–1295, May 1995.

[2] G. J. Huffman, R. F. Adler, P. Arkin, A. Chang, R. Ferraro, A. Gruber, J. Janowiak, A. McNab, B. Rudolf, and U. Schneider, "The Global Precipitation Climatology Project (GPCP) combined precipitation dataset," *Bull. Amer. Meteor. Soc.*, vol. 78, no. 1, pp. 5–20, Jan. 1997.

[3] G. J. Huffman, R. F. Adler, M. M. Morrissey, D. T. Bolvin, S. Curtis, R. Joyce, B. McGavock, and J. Susskind, "Global precipitation at one-degree daily resolution from multisatellite observations," *J. Hydrometeor.*, vol. 2, no. 1, pp. 36–50, Feb. 2001.

[4] R. F. Adler, G. J. Huffman, A. Chang, R. Ferraro, P. Xie, J. Janowiak, B. Rudolf, U. Schneider, S. Curtis, D. Bolvin, A. Gruber, J. Susskind, and P. Arkin, "The version 2 global precipitation climatology project (GPCP) monthly precipitation analysis (1979-present)," *J. Hydrometeor.*, vol. 4, no. 6, pp. 1147–1167, Dec. 2003.

[5] G. J. Huffman, R. F. Adler, D. T. Bolvin, G. Gu, E. J. Nelkin, K. P. Bowman, Y. Hong, E. F. Stocker, and D. B. Wolff, "The TRMM multi-satellite precipitation analysis: Quasi-global, multi-year, combined-sensor precipitation estimates at fine scale," *J. Hydrometeor.*, vol. 8, no. 1, pp. 38–55, Feb. 2007.

[6] R. Joyce, J. E. Janowiak, P. A. Arkin, and P. Xie, "CMORPH: A method that produces global precipitation estimates from passive microwave and infrared data at high spatial and temporal resolution," *J. Hydrometeor.*, vol. 5, no. 3, pp. 487–503, Jun. 2004.

[7] R. Joyce and P. Xie, "Kalman filter-based CMORPH," *J. Hydrometeor.*, vol. 12, no. 6, pp. 1547–1563, Dec. 2011.

[8] K. Hsu, A. Behrangi, B. Imam, and S. Sorooshian, "Extreme precipitation estimation using satellite-based PERSIANN-CCS algorithm," in *Satellite Rainfall Applications for Surface Hydrology*, M. Gebremichael and F. Hossain, Eds. New York, NY, USA: Springer-Verlag, 2010, pp. 3–22.

[9] S. Sorooshian, K. L. Hsu, X. Gao, H. V. Gupta, B. Imam, and D. Braithwaite, "Evaluation of PERSIANN system satellite—Based estimates of tropical rainfall," *Bull. Amer. Meteor. Soc.*, vol. 81, no. 9, pp. 2035–2046, Sep. 2000.

[10] A. Behrangi, B. Imam, K. L. Hsu, S. Sorooshian, T. J. Bellerby, and G. J. Huffman, "REFAME: Rain estimation using forward-adjusted advection of microwave estimates," *J. Hydrometeor.*, vol. 11, no. 6, pp. 1305–1321, Dec. 2010.

[11] T. Ushio, T. Kubota, S. Shige, K. Okamoto, K. Aonashi, T. Inoue, N. Takahashi, T. Iguchi, M. Kachi, R. Oki, T. Morimoto, and Z. Kawasaki, "A Kalman filter approach to the global satellite mapping of precipitation (GSMaP) from combined passive microwave and infrared radiometric data," *J. Meteor. Soc. Jpn.*, vol. 87A, pp. 137–151, 2009.

[12] J. T. Turk, G. V. Mostovoy, and V. Anantharaj, "The NRL-blend high resolution precipitation product and its application to land surface hydrology," in *Satellite Rainfall Applications for Surface Hydrology*, M. Gebremichael and F. Hossain, Eds. New York, NY, USA: Springer-Verlag, 2010, pp. 85–104.

[13] G. J. Huffman, R. F. Adler, D. T. Bolvin, and E. Nelkin, "The TRMM multi-satellite Precipitation Analysis (TMPA)," in *Satellite Rainfall Applications for Surface Hydrology*, M. Gebremichael and F. Hossain, Eds. New York, NY, USA: Springer-Verlag, 2010, pp. 3–22.

[14] C. Kidd, D. R. Kniveton, M. C. Todd, and T. J. Bellerby, "Satellite rainfall estimation using combined passive microwave and infrared algorithms," *J. Hydrometeor.*, vol. 4, no. 6, pp. 1088–1104, Dec. 2003.

[15] A. S. Gebregiorgis and F. Hossain, "How much can a priori hydrologic model predictability help in optimal merging of satellite precipitation products?" *J. Hydrometeor.*, vol. 12, no. 6, pp. 1287–1298, Dec. 2011.

[16] A. M. Ebtehaj and E. Foufoula-Georgiou, "Adaptive fusion of multisensor precipitation using Gaussian-scale mixtures in the wavelet domain," *J. Geophys. Res.*, vol. 116, no. D22, p. D22 110, Nov. 2011.

[17] E. E. Ebert, J. E. Janowiak, and C. Kidd, "Comparison of near real time precipitation estimates from satellite observations and numerical models," *Bull. Amer. Meteor. Soc.*, vol. 88, no. 1, pp. 47–64, Jan. 2007.

[18] Y. Tian, C. D. Peters-Lidard, B. J. Choudhury, and M. Garcia, "Multitemporal analysis of TRMM based satellite precipitation products for land data assimilation applications," *J. Hydrometeor.*, vol. 8, no. 6, pp. 1165–1183, Dec. 2007.

[19] Y. Tian and C. D. Peters-Lidard, "A global map of uncertainties in satellite-based precipitation measurements," *Geophys. Res. Lett.*, vol. 37, no. 24, p. L24 407, Dec. 2010.

[20] Y. Hong, K.-L. Hsu, H. Moradkhani, and S. Sorooshian, "Uncertainty quantification of satellite precipitation estimation and Monte Carlo assessment of the error propagation into hydrologic response," *Water Resour. Res.*, vol. 42, no. 8, p. W08 421, Aug. 2006.

[21] T. Ling, F. Hossain, and G. J. Huffman, "Transfer of satellite rainfall uncertainty from gauged to ungauged regions at regional and seasonal time scales," *J. Hydrometeorol.*, vol. 11, no. 6, pp. 1263–1274, Dec. 2010.

[22] G. J. Huffman, "Estimates of root mean square random error for finite samples of estimated precipitation," *J. Appl. Meteorol.*, vol. 36, no. 9, pp. 1191–1201, Sep. 1997.

[23] E. N. Anagnostou, W. F. Krajewski, and J. A. Smith, "Uncertainty quantification of mean-areal radar rainfall estimates," *J. Atmos. Ocean. Technol.*, vol. 16, no. 2, pp. 206–215, Feb. 1999.
[24] G. J. Ciach, E. Habib, and W. F. Krajewski, "Zero-covariance hypothesis in the error variance separation method of radar rainfall verification," *Adv. Water Resour.*, vol. 26, no. 5, pp. 573–580, May 2003.
[25] M. Gebremichael, W. F. Krajewski, M. Morrissey, D. Langerud, G. J. Huffman, and R. Adler, "Error uncertainty analysis of GPCP monthly rainfall products: A data-based simulation study," *J. Appl. Meteorol.*, vol. 42, no. 12, pp. 1837–1848, Dec. 2003.
[26] A. S. Gebregiorgis, Y. Tian, C. Peters-Lidard, and F. Hossain, "Tracing hydrologic model simulation error as a function of satellite rainfall estimation bias components and land use and land cover conditions," *Water Resources Res.*, vol. 48, no. 11, p. W11 509, Nov. 2012.
[27] A. S. Gebregiorgis and F. Hossain, "Understanding the dependency of satellite rainfall uncertainty on topography and climate for hydrologic model simulation," *IEEE Trans. Geosci. Remote Sens.*, vol. 51, no. 1, pp. 704–718, Jan. 2013.
[28] F. Hossain, E. N. Anagnostou, and T. Dinku, "Sensitivity analyses of satellite rainfall retrieval and sampling error on flood prediction uncertainty," *IEEE Trans. Geosci. Remote Sens.*, vol. 42, no. 1, pp. 130–139, Jan. 2004.
[29] F. Hossain and E. N. Anagnostou, "Assessment of current passive-microwave- and infrared-based satellite rainfall remote sensing for flood prediction," *J. Geophys. Res.*, vol. 109, no. D7, p. D07 102, Apr. 2004.
[30] Q. Li, R. Ferraro, and N. C. Grody, "Detailed analysis of the error associated with the rainfall retrieved by the NOAA/NESDIS SSM/I rainfall algorithm: 1. Tropical oceanic rainfall," *J. Geophys. Res.*, vol. 103, no. D10, pp. 11 419–11 427, May 1998.
[31] J. R. McCollum and W. F. Krajewski, "Investigations of error sources of the global precipitation climatology project emission algorithm," *J. Geophys. Res.*, vol. 103, no. D22, pp. 28 711–28 719, Jan. 1998.
[32] B. Nijssen and D. P. Lettenmaier, "Effect of precipitation sampling error on simulated hydrological fluxes and states: Anticipating the global precipitation measurement satellites," *J. Geophys. Res.*, vol. 109, no. D2, p. D02 103, Jan. 2004.
[33] B. Rudolf, "Management and analysis of precipitation data on a routine basis," in *Proc. Int. WMO/IAHS/ETH Symp. Precipitation Evap.*, M. Lapin and B. Sevruk, Eds., Bratislava, Slovakia, 1993, vol. 1, pp. 69–76.
[34] M. Steiner, "Uncertainty of estimates of monthly areal rainfall for temporally sparse remote observations," *Water Resour. Res.*, vol. 32, no. 2, pp. 373–388, Jan. 1996.
[35] M. Steiner, J. A. Smith, S. J. Burges, C. V. Alonso, and R. W. Darden, "Effect of bias adjustment and rain gauge data quality control on radar rainfall estimation," *Water Resour. Res.*, vol. 35, no. 8, pp. 2487–2503, Jan. 1999.
[36] M. Steiner, T. L. Bell, Y. Zhang, and E. F. Wood, "Comparison of two methods for estimating the sampling-related uncertainty of satellite rainfall averages based on a large radar data set," *J. Climate*, vol. 16, no. 22, pp. 3759–3778, Nov. 2003.
[37] Y. Tian, C. D. Peters-Lidard, J. B. Eylander, R. J. Joyce, G. J. Huffman, R. F. Adler, K. Hsu, F. J. Turk, M. Garcia, and J. Zeng, "Component analysis of errors in satellite-based precipitation estimates," *J. Geophys. Res.*, vol. 114, no. D24, p. D24 101, Dec. 2009.
[38] M. Gebremichael and W. Krajewski, "Characterization of the temporal sampling error in space–time-averaged rainfall estimates from satellites," *J. Geophys. Res.*, vol. 109, no. D11, p. D11 110, Jun. 2004.
[39] A. S. Gebregiorgis and F. Hossain, "Performance evaluation of merged satellite rainfall products based on spatial and seasonal signatures of hydrologic predictability," *Atmosp. Res.*, 2013, to be published.
[40] M. Widmann, C. S. Bretherton, and R. P. Salathe, "Statistical precipitation downscaling over the northwestern united states using numerically simulated precipitation as a predictor," *J. Climate*, vol. 16, no. 5, pp. 799–816, Mar. 2002.
[41] E. P. Maurer, A. W. Wood, J. C. Adam, D. P. Lettenmaier, and B. Nijssen, "A long-term hydrologically based dataset of land surface fluxes and states for the conterminous united states," *J. Climate*, vol. 15, no. 22, pp. 3237–3251, Nov. 2002.
[42] C. G. Rossi, T. J. Dybala, D. N. Moriasi, J. G. Arnold, C. Amonett, and T. Marek, "Hydrologic calibration and validation of the soil and water assessment tool for the Leon River watershed," *Soil Water Conserv.*, vol. 63, no. 6, pp. 533–541, Nov./Dec. 2008.

Abebe S. Gebregiorgis received the B.Sc. degree in hydraulic engineering from Arba Minch Water Technology Institute, Arba Minch, Ethiopia, in 2002 and the M.Sc. degree in hydraulic and hydropower engineering from Arba Minch University, Arba Minch, in 2004. He is currently working toward the Ph.D. degree at Tennessee Technological University, Cookeville, TN, in civil and environmental engineering.

His field of research is on hydrologically relevant and optimal merging of high resolution satellite precipitation products to enhance macroscale hydrologic modeling application. He is also one of the winners of the prestigious NASA Earth and Space Science Fellowship for 2012.

Faisal Hossain received B.S. degree from the Indian Institute of Technology, Varanasi, India, the M.S. degree from The National University of Singapore, Singapore, and the Ph.D. degree from The University of Connecticut, Storrs, CT, in 2004.

He is currently an Associate Professor in the Department of Civil and Environmental Engineering where he received one of highest awards of University—the Caplenor Research Award in 2012. His research interests comprise hydrologic remote sensing, uncertainty modeling of water cycle variables, human modification of extreme hydro-climatology, sustainable water resources engineering, space-borne transboundary water resources management, engineering education and public outreach. He has published over 85 peer-reviewed journal articles, authored an undergraduate-level textbook, edited two book volumes and contributed eight book chapters. His recent research on human modification of extreme events by artificial reservoirs has been featured by public media such as the BBC, National Geographic, New Scientist, Newsweek, Fox News, MSNBC, Wired.com and German Public Radio. He served as Associate Editor of the *Journal of American Water Resources Association* from 2006 to 2010. Currently, he serves as an Associate Editor for the *Journal of Hydrometeorology* and Lead Editor for the water volume of Elsevier Sciences 5 volume reference series on *Climate Vulnerability: Understanding and Addressing Threats to Essential Resources.*

Dr. Hossain is also the recipient of awards such as NASA Earth System Science Fellowship (2002), Outstanding PhD Thesis Award (2005), NASA New Investigator Award (2008), American Society of Engineering Education (ASEE) Outstanding Research Award (2009), National Association of Environmental Professionals Education Excellence Award (2010), US Fulbright Faculty Award (2012), G.O.L.D. (Graduate Of the Last Decade) award from University of Connecticut (2012) and American Geophysical Union (AGU) Charles Falkenberg Award.